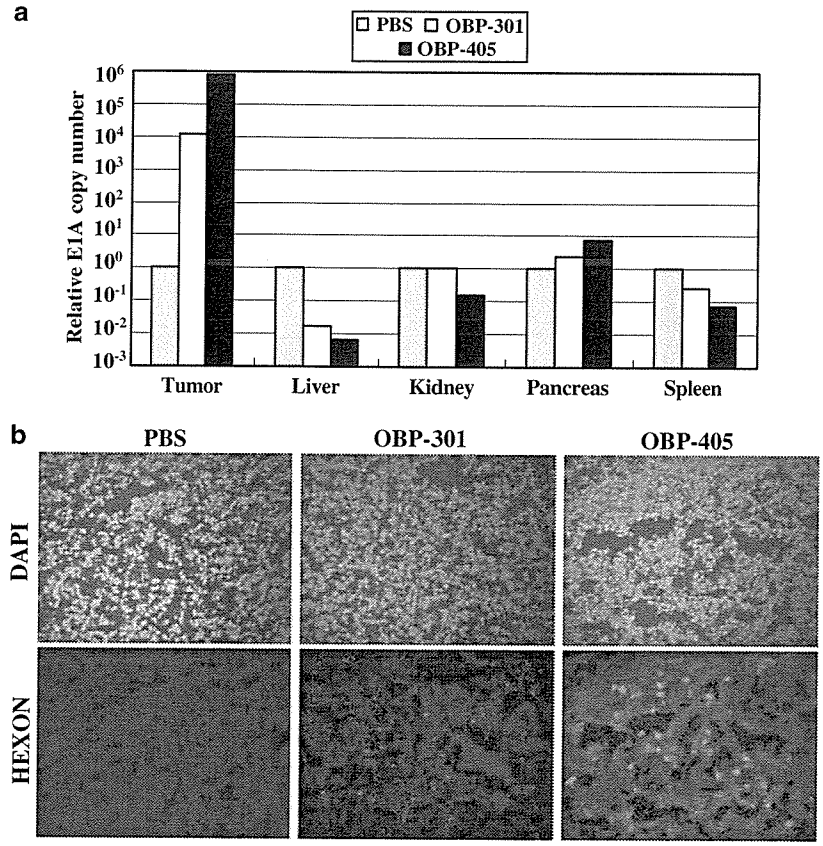

Figure 6 Spread and replication of OBP-301 or OBP-405 following intratumoral administration in *nu/nu* mice transplanted with H1299-R5 tumor cells. **(a)** DNA was extracted from subcutaneous tumor and various tissues in *nu/nu* mice at 7 day postinfection. Viral DNA was detected by quantitative PCR amplification of the adenoviral E1A sequence. The amounts of viral E1A copy number are defined as the fold increase for each sample relative to that with PBS (PBS equals 1). The results are representative of three separate experiments. **(b)** Sections of H1299-R5 tumors were immunofluorescently stained with anti-hexon antibody 7 days after virus injection, followed by counterstaining with DAPI. Magnification, × 200

Table 1 Assessment of hepatotoxicity in *nu/nu* mice intratumorally injected with OBP-301 or OBP-405

	T-Bil (mg/dl)	*AST (IU/l)*	*ALT (IU/l)*	*LDH (IU/l)*	*GGT (IU/l)*	*ALP (IU/l)*
PBS	0.4	87	31	258	< 10	475
OBP-301	0.3	118	40	388	< 10	382
OBP-405	0.4	69	27	190	< 10	492

Blood was obtained from H1299-R5 tumor-bearing mice 7 days after intratumoral injection of PBS or 1×10^7 PFU of OBP-301 or OBP-405, and the levels of liver enzymes were analysed

adenoviruses (Ginsberg *et al.*, 1991; Prince *et al.*, 1993). However, as preliminary data, we confirmed that OBP-405 could infect and efficiently lyse murine adenocarcinoma cell line Colon-26 (data not shown). Therefore, OBP-405 is considered to be specific and safe within its therapeutic window.

To treat distant, metastatic tumors, an infusion of chemotherapeutic drugs by intravenous administration will need to distribute a sufficient quantity of agents to the tumor sites; oncolytic viruses, however, could replicate in the tumor, cause oncolysis, and then release virus particles that will reach to the distant metastatic lesions. Therefore, intratumoral administration that causes the release of newly formed virus from infected tumor cells might be theoretically suitable for oncolytic virus rather than systemic administration. OBP-405 cleared rapidly from the body after intravenous administration (data not shown). This is one of the reasons why we also used intratumoral injection of OBP-405 for the toxicity analysis. In fact, a phase I clinical study demonstrated PSA-specific oncolytic virus shedding in the blood after intraprostatic delivery (DeWeese *et al.*,

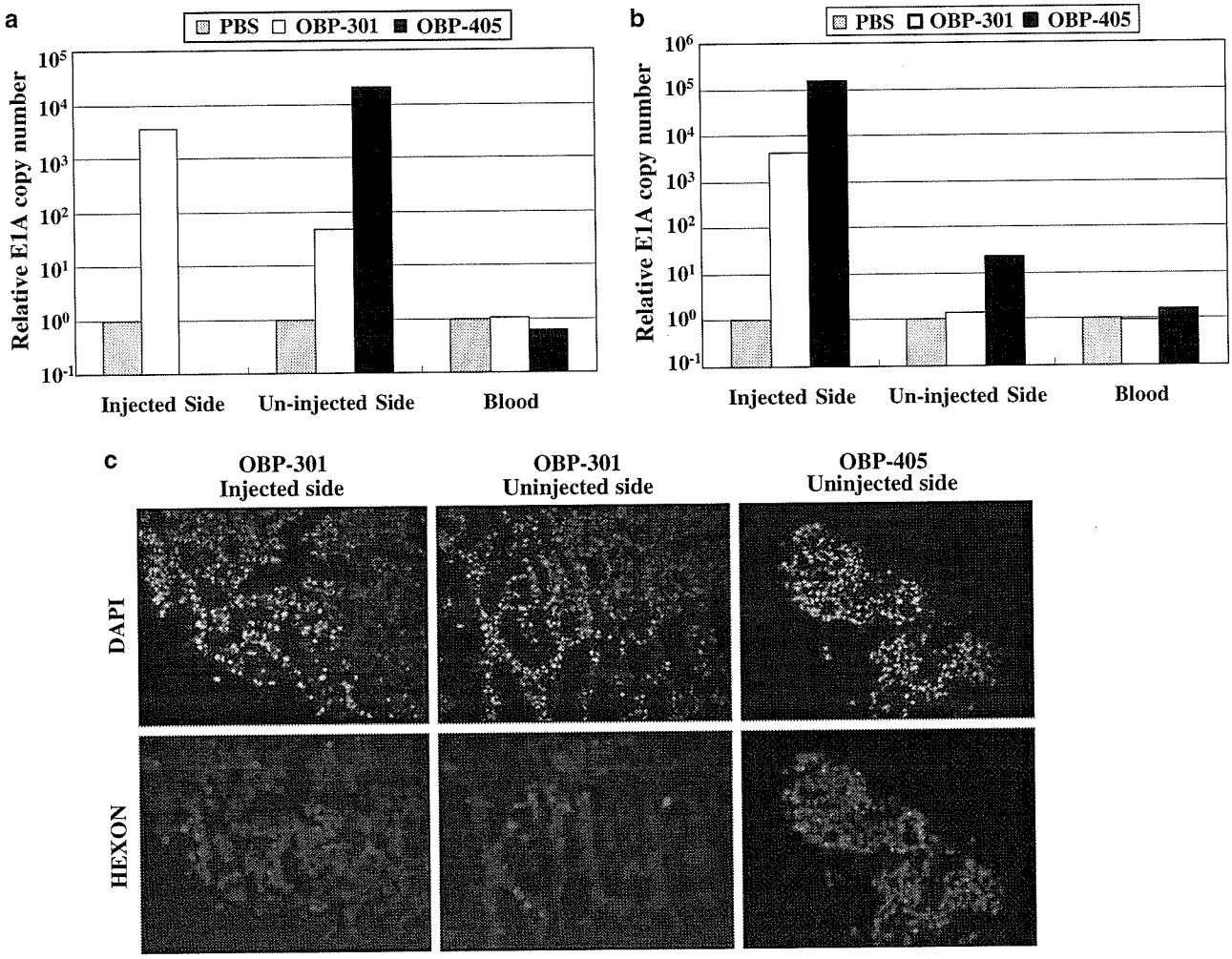

Figure 7 Replication of OBP-301 and OBP-405 in the tumor distant from the site of virus inoculation. Bilateral H1299-R5 tumors were implanted in *nu/nu* mice, and the right-sided tumors received intratumoral injection of PBS or 1×10^7 PFU of OBP-301 or OBP-405. The results are representative of three separate experiments. **(a, b)** Quantitative real-time PCR amplification of the E1A gene with DNA isolated from the right (injected) and left (uninjected) H1299-R5 tumors at 2 weeks **(a)** and 1 month **(b)** post-treatment. **(c)** Sections of H1299-R5 tumors were immunofluorescently stained with anti-hexon antibody 1 month after virus injection, followed by counterstaining with DAPI. Magnification, $\times 200$

2001). These findings indicate that the intratumorally administered virus that reached the circulation could potentially replicate and lyse metastatic tumors. We observed evidence of OBP-405 replication in the distant, uninjected H1299-R5 tumors after its intratumoral administration into the contralateral tumors by quantification of virus DNA (Figure 7). Moreover, OBP-405 continued to replicate in the distant tumors even after the injected tumors disappeared, although the presence of OBP-405 in the blood circulation could not be detected over time. One possible explanation for this result is that the amount of OBP-405 in the circulation might be quite small due to its short half-life (approximately 2 min) (Huard *et al.*, 1995; Wood *et al.*, 1999), but sufficient to initiate replication once it reached the distant tumors.

In conclusion, we demonstrate that the fiber-modified telomerase-specific replication-selective adenovirus OBP-405 permits CAR-independent cell entry and effective destruction of tumors lacking the primary CAR. The feasibility of original OBP-301 (Telomelysin) for human cancer therapy will be confirmed in clinical trials in the near future; some CAR-negative tumors, however, may be refractory to OBP-301. Under such circumstances, OBP-405 is a powerful way of overcoming low infectivity and increasing antitumor activity. Our data may be consequential for the development of virotherapy for human cancers.

Materials and methods

Cells and culture conditions

The H1299 and H1299-R5 human non-small-cell lung cancer cell lines and the SW620 human colon cancer cell line were cultured in RPMI 1640 medium supplemented with 10% FCS. H1299-R5 is a subline of H1299 that are refractory to adenovirus infection due to the decreased CAR expression

(Tango *et al.*, 2004). The human glioma cell lines LN444 and LNZ308 (kindly provided by Dr N Ishi, Hokkaido University, Hokkaido, Japan), and the transformed embryonic kidney cell line 293 were cultured in DMEM containing high glucose (4.5 g/l) and supplemented with 10% FCS. The normal human lung fibroblast cell line NHLF was purchased from TaKaRa Biomedicals (Kyoto, Japan) and cultured in the medium recommended by the manufacturer.

Recombinant adenoviruses

The recombinant replication-selective, tumor-specific adenovirus vector OBP-301 ('Telomelysin') was previously constructed and characterized (Kawashima *et al.*, 2004; Umeoka *et al.*, 2004). OBP-405 ('Telomelysin-RGD') that has mutant fiber containing the RGD peptide, CDCRGDCFC, in the HI loop of the fiber knob was created using the method developed by Mizuguchi *et al.* (2001). OBP-301 and OBP-405 viruses were purified by $CsCl_2$ step gradient ultracentrifugation followed by $CsCl_2$ linear gradient ultracentrifugation. Determination of virus particle titer and infectious titer was accomplished spectrophotometrically by the method of Maizel *et al.* (1968) and by the method of Kanegae *et al.* (1994), respectively.

Flow cytometry

The cells (2×10^5 cells) were labeled with mouse monoclonal anti-CAR (RmcB; Upstate Biotechnology, NY, USA), anti-human integrin $\alpha v\beta 3$ (LM609; Chemicon International, Temecula, CA, USA), or anti-human integrin $\alpha v\beta 5$ (P1F6; Chemicon International, Temecula, CA, USA). Then, the cells were incubated with FITC-conjugated rabbit anti-mouse IgG second antibody (Zymed Laboratories, San Francisco, USA) and analysed by flow cytometry (FACScan, Becton Dickinson, Mountain View, CA, USA).

Quantitative real-time PCR assay

DNA was extracted with QIAamp DNA Mini Kit (Qiagen Inc., Valencia, CA, USA), and quantitative real-time PCR assay for the E1A gene was performed using a LightCycler instrument (Roche Molecular Biochemicals, Indianapolis, IN, USA). The sequences of specific primers used for E1A were as follows: sense: 5′-CCT GTG TCT AGA GAA TGC AA-3′ and antisense: 5′-ACA GCT CAA GTC CAA AGG TT-3′). PCR amplification began with a 600-s denaturation step at 95°C and then 40 cycles of denaturation at 95°C for 10 s, annealing at 58°C for 15 s, and extension at 72°C for 8 s. Data analysis was performed using LightCycler Software (Roche Molecular Biochemicals). The ratios normalized by dividing the value of untreated cells were presented for each sample.

Viral spread assay

H1299, LN444, and NHLF were cultured in two-well chamber slides and infected with OBP-301 or OBP-405 at an MOI of 1. The slides were fixed with 4% paraformaldehyde 24 or 48 h after infection, blocked, incubated with FITC-labeled goat anti-hexon polyclonal antibody (25 μg/ml; Chemicon Inc., Temecula, CA, USA), and counterstained with DAPI (1 μg/ml; Molecular Probes, Eugene, OR, USA). The slides were photographed under the fluorescence microscopy and then analysed using the software (Viewfinder; Pixera, CA, USA).

Cell killing assay

Cells were plated at 100 000 cells/well on 12-well plates and infected either with OBP-301 or OBP-405 at an MOI of 0, 0.1, or 1 for 2 h. The medium with 10% FBS was then added following the removal of viruses. Coomassie brilliant blue staining was performed on day 5.

Cell viability assay

An XTT assay was performed to measure cell viability. Cells were plated on 96-well plates at 5×10^3/well, 24 h before infection and infected either with OBP-301 or OBP-405 at an MOI of 0, 0.1, or 1. Cell viability was determined at the indicated times by using a Cell Proliferation Kit II (Roche Molecular Biochemicals) according to the manufacturer's protocol.

In vivo *human tumor model*

Human lung cancer H1299-R5 cells (1×10^7 cells/mouse) were subcutaneously injected into the flank of 5–6-week-old female BALB/c *nu/nu* mice and permitted to grow to approximately 5–6 mm in diameter. At that time, the mice were randomly assigned into four groups, and a 100 μl solution containing 1×10^7 PFU of dl312, OBP-301, or OBP-405, or PBS was injected into the tumor on days 1, 2, and 3. Tumors were measured for perpendicular diameters every 3 or 4 days, and tumor volume was calculated using the following formula: tumor volume $(mm^3) = a \times b^2 \times 0.5$, where a is the longest diameter, b is the shortest diameter, and 0.5 is a constant to calculate the volume of an ellipsoid. The experimental protocol was approved by the Ethics Review Committee for Animal Experimentation of Okayama University Graduate School of Medicine and Dentistry.

In vivo *toxicity study*

Mice bearing H299-R5 tumors received intratumoral injection of 1×10^7 PFU of OBP-301 or OBP-405, or PBS. At 1 week after treatment, blood samples were obtained and the serum levels of total bilirubin (T-Bil), aspartate amino transferase (AST), alanine amino transferase (ALT), lactate dehydrogenase (LDH), gamma glutamyl transpeptidase (GGT), and alkaline phosphatase (ALP) were determined by automated colorimetric assays to assess the hepatotoxicity.

In vivo *viral replication*

OBP-301 or OBP-405 at 1×10^7 PFU/100 μl, or PBS were intratumorally injected into H1299-R5-bearing mice. After 1 week, the tumors and organs were harvested and DNA was extracted from each tissue. To compare the viral replication in the tumor and other normal organs, quantitative real-time PCR for the E1A gene was performed with a LightCycler instrument. The tumors and organs were immediately embedded in Tissue Tek (Sakura, Tokyo, Japan), cut into 5 μm-thick sections, and assessed by immunofluorescence detection of the adenoviral hexon protein using a goat anti-hexon polyclonal antibody (Chemicon, Temecula, CA, USA). To assess the viral replication on distant, uninjected tumors, H1299-R5 cells (1×10^7 cells/mouse) were injected subcutaneously into bilateral flanks of mice. At 2 weeks or 1 month after intratumoral inoculation of OBP-301 or OBP-405 at 1×10^7 PFU/100 μl into tumors in the right flank, the bilateral tumors and blood were collected from mice and DNA was extracted. Quantitative real-time PCR as well as immunofluorescence staining for the hexon protein were performed.

Statistical analysis

Determinations of significant differences among groups were assessed by calculating the value of Student's t using the original data analysis.

Abbreviations

hTERT, human telomerase reverse transcriptase; IRES, internal ribosome entry site; CAR, Coxsackie-adenovirus receptor; NHLF, normal human lung fibroblasts; MOI, multiplicity of infection; PFU, plaque-forming units.

Acknowledgements

We thank Yoshiko Shirakiya, Nobue Mukai, and Yuri Hashimoto (Oncolys BioPharma, Inc.) for their excellent technical support. This work was supported in part by grants from the Ministry of Education, Science and Culture, Japan; and by grants from the Ministry of Health and Welfare, Japan.

References

Bergelson JM, Cunningham JA, Droguett G, Kurt-Jones EA, Krithivas A, Hong JS, Horwitz MS, Crowell RL and Finberg RW. (1997). *Science*, **275,** 1320–1323.

Collins K and Mitchell JR. (2002). *Oncogene*, **21,** 564–579.

Davydova J, Le LP, Gavrikova T, Wang M, Krasnykh V and Yamamoto M. (2004). *Cancer Res.*, **64,** 4319–4327.

DeWeese TL, van der Poel H, Li S, Mikhak B, Drew R, Goemann M, Hamper U, DeJong R, Detorie N, Rodriguez R, Haulk T, DeMarzo AM, Piantadosi S, Yu DC, Chen Y, Henderson DR, Carducci MA, Nelson WG and Simons JW. (2001). *Cancer Res.*, **61,** 7464–7472.

Dmitriev I, Krasnykh V, Miller CR, Wang M, Kashentseva E, Mikheeva G, Belousova N and Curiel DT. (1998). *J. Virol.*, **72,** 9706–9713.

Fang B and Roth JA. (2003). *Curr. Opin. Mol. Ther.*, **5,** 475–482.

Fechner H, Wang X, Wang H, Jansen A, Pauschinger M, Scherubl H, Bergelson JM, Schultheiss HP and Poller W. (2000). *Gene Ther.*, **7,** 1954–1968.

Ginsberg HS, Moldawer LL, Sehgal PB, Redington M, Kilian PL, Chanock RM and Prince GA. (1991). *Proc. Natl. Acad. Sci. USA*, **88,** 1651–1655.

Greider CW and Blackburn EH. (1985). *Cell*, **43,** 405–413.

Gu J, Kagawa S, Takakura M, Kyo S, Inoue M, Roth JA and Fang B. (2000). *Cancer Res.*, **60,** 5359–5364.

Gu J, Zhang L, Huang X, Lin T, Yin M, Xu K, Ji L, Roth JA and Fang B. (2002). *Oncogene*, **21,** 4757–4764.

Hemminki A, Kanerva A, Liu B, Wang M, Alvarez RD, Siegal GP and Curiel DT. (2003). *Cancer Res.*, **63,** 847–853.

Huard J, Lochmuller H, Acsadi G, Jani A, Massie B and Karpati G. (1995). *Gene Ther.*, **2,** 107–115.

Kanegae Y, Makimura M and Saito I. (1994). *Jpn. J. Med. Sci. Biol.*, **47,** 157–166.

Kawashima T, Kagawa S, Kobayashi N, Shirakiya Y, Umeoka T, Teraishi F, Taki M, Kyo S, Tanaka N and Fujiwara T. (2004). *Clin. Cancer Res.*, **10,** 285–292.

Kim NW, Piatyszek MA, Prowse KR, Harley CB, West MD, Ho PL, Coviello GM, Wright WE, Weinrich SL and Shay JW. (1994). *Science*, **266,** 2011–2015.

Kirn D, Martuza RL and Zwiebel J. (2001). *Nat. Med.*, **7,** 781–787.

Koga S, Hirohata S, Kondo Y, Komata T, Takakura M, Inoue M, Kyo S and Kondo S. (2000). *Hum. Gene Ther.*, **11,** 1397–1406.

Kohn EC, Lu Y, Wang H, Yu Q, Yu S, Hall H, Smith DL, Meric-Bernstam F, Hortobagyi GN and Mills GB. (2004) **31,** 39–53.

Komata T, Kondo Y, Kanzawa T, Hirohata S, Koga S, Sumiyoshi H, Srinivasula SM, Barna BP, Germano IM, Takakura M, Inoue M, Alnemri ES, Shay JW, Kyo S and Kondo S. (2001). *Cancer Res.*, **61,** 5796–5802.

Krasnykh V, Dmitriev I, Mikheeva G, Miller CR, Belousova N and Curiel DT. (1998). *J. Virol.*, **72,** 1844–1852.

Lamfers ML, Grill J, Dirven CM, Van Beusechem VW, Geoerger B, Van Den Berg J, Alemany R, Fueyo J, Curiel DT, Vassal G, Pinedo HM, Vandertop WP and Gerritsen WR. (2002). *Cancer Res.*, **62,** 5736–5742.

Li Y, Pong RC, Bergelson JM, Hall MC, Sagalowsky AI, Tseng CP, Wang Z and Hsieh JT. (1999). *Cancer Res.*, **59,** 325–330.

Maizel JVJ, White DO and Scharff MD. (1968). *Virology*, **36,** 115–125.

McCormick F. (2001). *Nat. Rev. Cancer*, **1,** 130–141.

Miller CR, Buchsbaum DJ, Reynolds PN, Douglas JT, Gillespie GY, Mayo MS, Raben D and Curiel DT. (1998). *Cancer Res.*, **58,** 5738–5748.

Mizuguchi H, Koizumi N, Hosono T, Utoguchi N, Watanabe Y, Kay MA and Hayakawa T. (2001). *Gene Ther.*, **8,** 730–735.

Nakamura TM, Morin GB, Chapman KB, Weinrich SL, Andrews WH, Lingner J, Harley CB and Cech TR. (1997). *Science*, **277,** 955–959.

Prince GA, Porter DD, Jenson AB, Horswood RL, Chanock RM and Ginsberg HS. (1993). *J. Virol.*, **67,** 101–111.

Shay JW and Wright WE. (1996). *Curr. Opin. Oncol.*, **8,** 66–71.

Tango Y, Taki M, Shirakiya Y, Ohtani S, Tokunaga N, Tsunemitsu Y, Kagawa S, Tani T, Tanaka N and Fujiwara T. (2004). *Cancer Sci.*, **95,** 459–643.

Tomko RP, Xu R and Philipson L. (1997). *Proc. Natl. Acad. Sci. USA*, **94,** 3352–3356.

Umeoka T, Kawashima T, Kagawa S, Teraishi F, Taki M, Nishizaki M, Kyo S, Nagai K, Urata Y, Tanaka N and Fujiwara T. (2004). *Cancer Res.*, **64,** 6259–6265.

Wickham TJ, Mathias P, Cheresh DA and Nemerow GR. (1993). *Cell*, **73,** 309–319.

Wickham TJ, Tzeng E, Shears II LL, Roelvink PW, Li Y, Lee GM, Brough DE, Lizonova A and Kovesdi I. (1997). *J. Virol.*, **71,** 8221–8229.

Wood M, Perrotte P, Onishi E, Harper ME, Dinney C, Pagliaro L and Wilson DR. (1999). *Cancer Gene Ther.*, **6,** 367–372.

Available online at www.sciencedirect.com
SCIENCE DIRECT®
Bioorganic & Medicinal Chemistry Letters
ELSEVIER
Bioorganic & Medicinal Chemistry Letters 15 (2005) 621–624

Design and synthesis of a peptide-PEG transporter tool for carrying adenovirus vector into cells☆

Mitsuko Maeda,[a] Shinya Kida,[a] Keiko Hojo,[a] Yusuke Eto,[b] Jian-Qing Gaob,[b] Shinnosuke Kurachi,[b] Fumiko Sekiguchi,[b] Hiroyuki Mizuguchi,[c] Takao Hayakawa,[d] Tadanori Mayumi,[a] Shinsaku Nakagawa[b] and Koichi Kawasaki[a,*]

[a]*Faculty of Pharmaceutical Sciences, Kobe Gakuin University, Nishi-ku, Kobe 651-2180, Japan*
[b]*Graduate School of Pharmaceutical Sciences, Osaka University, Yamadaoka, Suita 565-0871, Japan*
[c]*Division of Cellular and Gene Therapy Products, National Institute of Health Sciences, Setagaya-ku, Tokyo 158-8501, Japan*
[d]*National Institute of Health Sciences, Setagaya-ku, Tokyo 158-8501, Japan*

Received 17 September 2004; accepted 16 November 2004
Available online 23 December 2004

Abstract—The adenovirus vector is a promising carrier for the efficient transfer of genes into cells via the coxackie-adenovirus receptor (CAR) and integrins (αvβ3 and αvβ5). The clinical use of the adenovirus vector remains problematic however. Successful administration of this vector is associated with side effects because antibodies to this vector are commonly found throughout the human body. To make the adenovirus vector practicable for clinical use, it is necessary to design an auxiliary transporter. The present study describes the use of Arg-Gly-Asp(RGD)-related peptide, a peptide that binds to integrins, as an auxiliary transporter to aid efficient transport of adenovirus vector. Furthermore, poly(ethylene glycol) (PEG) was also used as a tool to modify the adenovirus such that the risk of side effects incurred during clinical application was reduced. The present study describes the design, preparation and use of (acetyl-Tyr-Gly-Gly-Arg-Gly-Asp-Thr-Pro-$_{\beta}$Ala)$_2$Lys-PEG-$_{\beta}$Ala-Cys-NH_2[(Ac-YGGRGDTP$_{\beta}$A)$_2$K-PEG-$_{\beta}$AC] as an efficient peptide-PEG transporter tool for carrying adenovirus vector into cells. (Ac-YGGRGDTP$_{\beta}$A)$_2$K-PEG-$_{\beta}$AC was coupled with 6-maleimidohexanoic acid *N*-hydroxysuccinimide ester and the resulting 6-[(Ac-YGGRGDTP$_{\beta}$A)$_2$K-PEG-$_{\beta}$AC-succinimido]hexanoic acid *N*-hydroxysuccinimide ester reacted with adenovirus. The modified adenovirus with the peptide-PEG hybrid exhibited high gene expression even in a CAR-negative cell line, DC2.4.

Gene therapy is a new field of clinical treatment for intractable diseases. A key aspect of gene therapy, and a major determinant of its success, lies in the vector used for transgenesis. Adenovirus vectors (Ad) are widely used as vectors for gene therapy experiments[2] since they exhibit highly efficient transduction and gene expression. Ad infection is performed in two steps; firstly Ad binds to its receptor, coxackie-adenovirus receptor (CAR),[3] followed by receptor-mediated endocytosis via αvβ3 and αvβ5 integrins.[4] Both of these integrins are known as a receptor of peptides containing the Arg-Gly-Asp (RGD) sequence. Ad is able to transfer genes efficiently into both dividing and nondividing cells, but some problems remain in terms of its clinical application. Side effects are common because antibodies to Ad are commonly found within the human body (Fig. 1).[5]

Poly(ethylene glycol) (PEG) is a low toxicity polymer and its hybrid formation (conjugation) with a protein is a method known to improve certain characteristics of the chosen protein (such as response to an antibody, response to enzymatic degradation, solubility to aqueous and organic solvents and prolongation of biological activities). As a result of this new methodology, the formation of a protein-PEG hybrid has become known as 'pegylation', a term that is now commonly used. Several studies have investigated the pegylation of Ad;[6] results demonstrated that pegylated Ad exhibited enhanced circulation and half-life in blood depending on the rate of pegylation. Transduction by the pegylated Ad was not disturbed in the presence of its antibody.[7] However the ability of the pegylated Ad to penetrate into cells

Keywords: Adenovirus vector; RGD; Poly(ethylene glycol); Transduction; Peptide synthesis.
☆See Ref. 1.
*Corresponding author. Tel.: +81 78 974 4794; fax: +81 78 974 5689; e-mail: kawasaki@pharm.kobegakuin.ac.jp

0960-894X/$ - see front matter © 2004 Elsevier Ltd. All rights reserved.
doi:10.1016/j.bmcl.2004.11.055

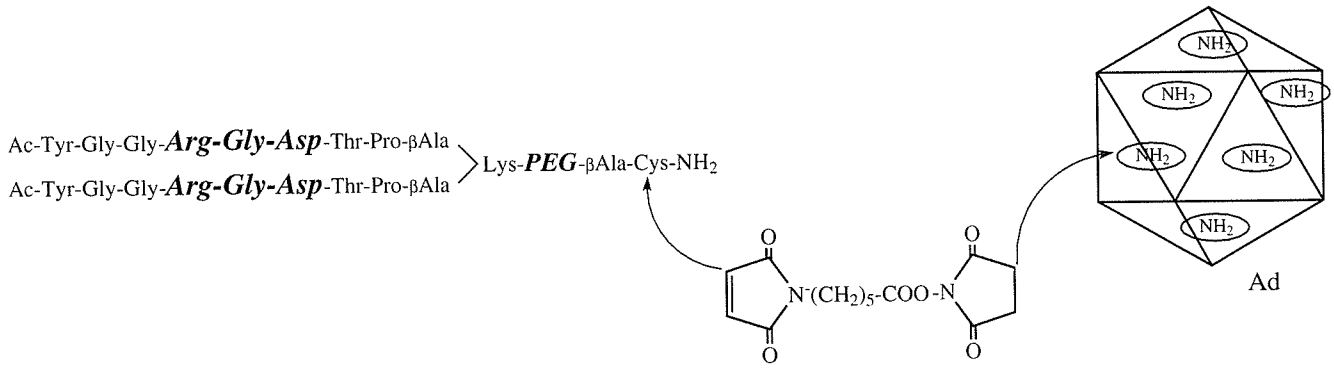

Figure 1. Design of an efficient peptide-PEG transporter tool for carrying adenovirus vector into cells via integrins.

through the coxackie-adenovirus receptor (CAR) was reduced by the steric hindrance of the associated PEG chains. To overcome this problem, an Arg-Gly-Asp(RGD)-related peptide, Tyr-Gly-Gly-Arg-Gly-Asp-Thr-Pro (YGGRGDTP),[8] was considered as a tool to allow Ad to penetrate into cells via its receptors (αvβ3 and αvβ5 integrins). The peptide was reported to show good endocytotic ability and RGD sequence in the peptide was reported to be necessary to exhibit this activity. Since the final synthetic product will be reacted with Ad by the active ester method, the RGD-related peptide should not have side chains, which will be acylated by the active ester method. YGGRGDTP has no such side chain (Fig. 2).

In an attempt to ensure efficient affinity between the peptide and integrins, a bivalent peptide derivative through Lys (K) was designed (Fig. 1). In order to prepare a hybrid of the peptide and PEG, an amino acid type PEG (aaPEG) was utilized. To introduce the peptide-PEG hybrid to Ad, a heterofunctional cross-linking reagent with amine and sulfhydryl reactivity, 6-maleim-

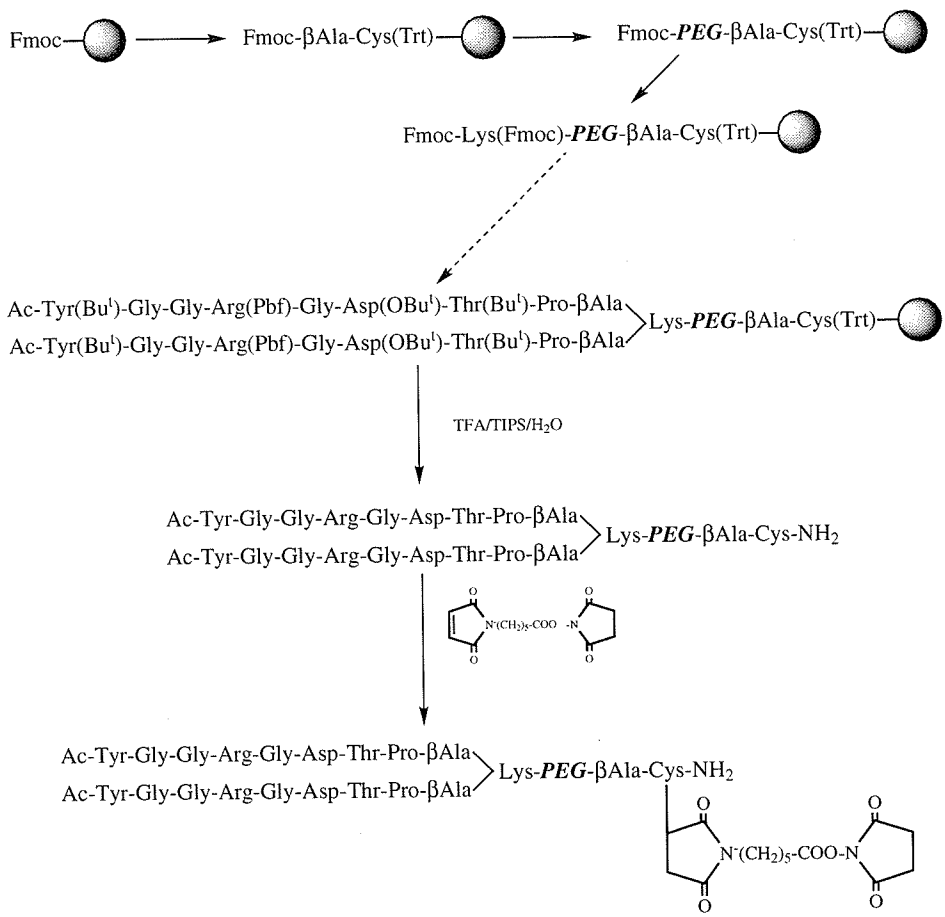

Figure 2. Synthetic scheme for the preparation of the PEG-(RGD-peptide) hybrid used to carry Ad into cells.

Table 1. Synthetic protocol for the solid-phase synthesis of Ac-YGGRGDTP)$_2$K-PEG-βAC

Step	Reagent	Volume	Period	Time
1	20% Piperidine/DMF	5 mL	5 min	1
		5 mL	0.5–1 h	1
2	DMF (wash)	5 mL	3 min	5
3	Fmoc-amino acid derivative	0.75 mmol		
	0.5 M HBTU/HOBt/DMF	1.5 mL	2–4 h	
	2 M DIEA/NMP	0.75 mL		
4	DMF (wash)	5 mL	3 min	5

idohexanoic acid *N*-hydroxysuccinimide ester[9] (MHS), was utilized. As a result, Cys was also incorporated in the hybrid. βAla (βA) was also incorporated into the hybrid as a spacer. The final hybrid, (acetyl-Tyr-Gly-Gly-Arg-Gly-Asp-Thr-Pro-βAla)$_2$Lys-PEG-βAla-Cys-NH_2, (Ac-YGGRGDTPβA)$_2$K-PEG-βAC amide, was thus designed (Fig. 2). The hybrid was synthesized by manual solid-phase methodology using fluorenylmethoxycarbonylamino acids (Fmoc-amino acids) on Rink amide resin (0.67 mequiv L/g, PE BioSystems. 370 mg, 0.25 mmol)[10] according to the protocol shown in Table 1. The following amino acids were purchased from Watanabe Chemical Industry Ltd (Japan) and Peptide Institute Inc. (Japan); Fmoc-Arg(Pbf)-OH (Pbf: 2,2,4,6,7-pentamethyldihydrobenzofuran-5-sulfonyl), Fmoc-Cys(Trt)-OH (Trt: trityl), Fmoc-Tyr(Bu^t)-OH (Bu^t: *tert*-butyl), Fmoc-Thr(Bu^t)-OH, Fmoc-Asp(OBu^t)-OH, N^{α},N^{ε}-diFmoc-Lys-OH, Fmoc-Gly-OH, Fmoc-βAla-OH and Fmoc-Pro-OH. Fmoc-aaPEG-OSu (–OSu: *N*-hydroxysuccinimide ester) (MW 3400) was purchased from Shearwater polymers Inc. and MHS was purchased from Dojindo Laboratories, Japan). All of the above materials were used as supplied without any further purification. As described in the protocol (Table 1), Fmoc groups were removed by 20% piperidine/dimethylformamide (DMF) treatment and coupling reactions were performed with 0.5 M 2-(1H-benzotriazole-1-yl)-1,1,3,3-tetramethyluronium hexafluorophosphate (HBTU)/DMF in the presence of 1-hydroxybenzotriazole (HOBt) in *N*-methylpyrrolidinone (NMP). Since Fmoc-aaPEG-OSu did not react with βAla-Cys(Trt)-Rink amide resin, HBTU, HOBt and diisopropylethylamine (DIEA) were added to the reaction mixture. The reaction did not proceed without the addition of HBTU, HOBt and DIEA. Since the deprotection reaction of the Fmoc group decreased in rate after the introduction of Fmoc-aaPEG, the following deprotection procedure was performed for 1 h. After the introduction of Lys, the amount of each added reagent was doubled, and each step involving the introduction of Fmoc-amino acid was performed using a double coupling reaction. The amino group of the *N*-terminal Tyr was acetylated with acetic anhydride. The synthetic (Ac-Tyr(Bu^t)-Gly-Gly-Arg(Pbf)-Gly-Asp-(OBu^t)-Thr(Bu^t)-Pro-βAla)$_2$Lys-aaPEG-βAla-Cys(Trt)-Rink amide resin was then treated with a mixture of trifluoroacetic acid (TFA)/H_2O/triisopropylsilane (TIPS) (95:2.5:2.5), and the resulting crude peptide-PEG hybrid, (Ac-YGGRGDTPβA)$_2$K-PEG-βAC, 462 mg), was purified by HPLC (Fig. 3). The purified hybrid (55 mg, 10 mmol)[11] dissolved in PBS (pH 7.4, 1 mL), and the

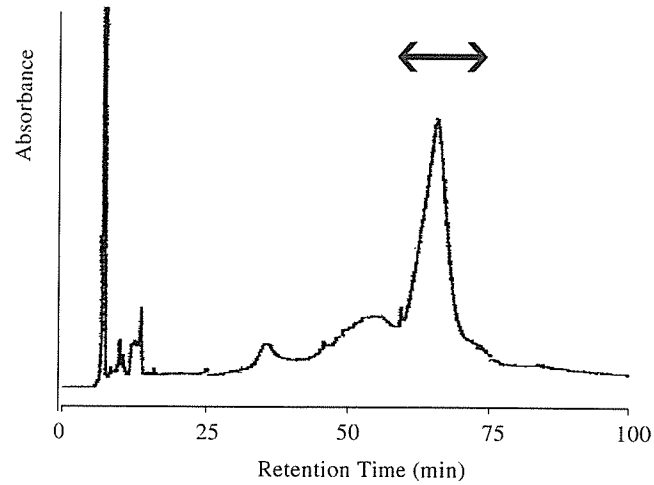

Figure 3. HPLC profile of synthetic crude (Ac-YGGRGDTPβA)$_2$K-PEG-βAC-SHS. Column: DAISOPAK SP-120-5-ODS-B (20 × 250 mm). Flow rate: 10 mL/min. Eluent: CH_3CN/H_2O containing 0.05% CF_3COOH. Gradient: 10:90 → 70:30 (60 min). OD at 220 nm.

heterofunctional cross-linkage reagent (MHS 3.1 mg, 10 mmol) dissolved in dimethylsulfoxide (DMSO, 0.1 mL), were combined and the mixture stirred for 0.5 h. Since the product of this reaction, [(Ac-YGGRGDTPβA)$_2$K-PEG-βAC-SHS)] (SHS: 6-succimidohexanoic acid *N*-hydroxysuccinimide ester) was easily hydrolyzed in water, the reaction mixture was frozen immediately and kept in a freezer to await the next reaction step. Purification of the reaction product by HPLC was attempted, but was not successful since the *N*-hydroxysuccinimide ester portion of the product hydrolysed easily in the presence of water. We observed that 50% of MHS was hydrolyzed at pH 7.4 after 1.5 h at room temperature (Fig. 4). Ad, which has luciferase expression ability, was modified with (Ac-YGGRGDTPβA)$_2$K-PEG-βAC-SHS solution at 37 °C for 45 min with gentle stirring and the transduction efficiency of the resulting modified Ad (RGDpep-PEG-Ad) via receptor-mediated endocytosis was examined with A549 (CAR + and integrins-positive) and DC2.4 (CAR – and integrins-positive) cell lines using a Luciferase Assay System Kit (Promege, USA) and a Microlumat Plus LB 96 instrument (Perkin–Elmer, USA), after

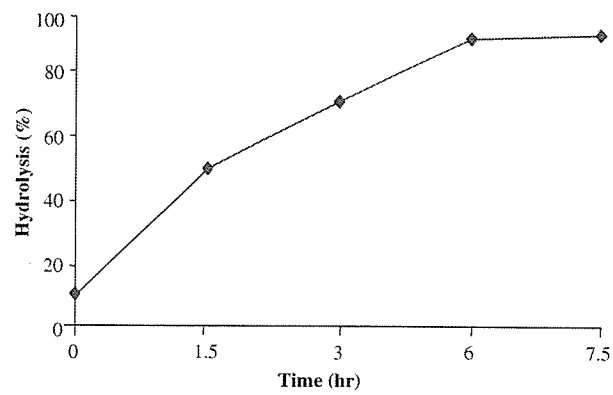

Figure 4. Hydrolysis of 6-maleimidohexanoic acid *N*-hydroxysuccinimide ester (MHS) in water at pH 7.4.

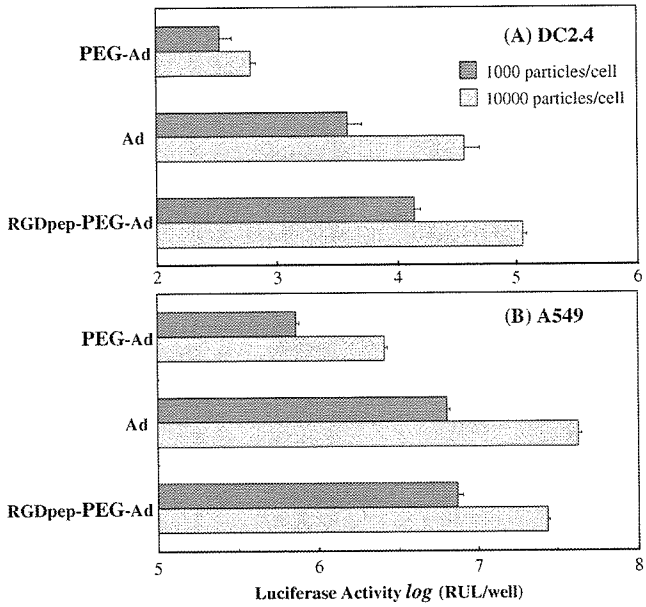

Figure 5. Transduction efficiency of RGDpep-PEG-Ad into DC2.4 (CAR −) cells and A549 (CAR +) cells. (A) DC2.4 cells (2×10^{10} cells) and (B) A549 cells (2×10^{10} cells) were transduced with 1000 and 10,000 particles/cells of Ad, PEG-Ad and RGDpep-PEG-Ad, respectively. Luciferase expression was measured after 24 h. Each point represents mean ± SD ($n = 3$).

cells were first lysed with Luciferase Cell Culture Lysis Reagent (Promega, USA). Luciferase activity was described as relative light unit per well (RLU/well). We thus measured the luciferase activity of cells transducted with Ad, PEG-Ad[7] RGDpep-PEG-Ad, as shown in Figure 5. A549 cells that had been infected with Ad or RGDpep-PEG-Ad exhibited luciferase activity in similar proportions. On the other hand, the luciferase activity of DC2.4 cells that had been infected with Ad was much lower than that of DC2.4 cells that had been infected with RGDpep-PEG-Ad. Furthermore, infection of cells with RGDpep-PEG-Ad was not blocked in the presence of an antibody to Ad (data is not shown). These results indicate that RGDpep-PEG-Ad could be transducted into cells via the integrins and was protected from the antibody by its pegylated structure.

In summary, we designed and prepared (Ac-YGGRGDTP$_\beta$A)$_2$K-PEG-$_\beta$AC as an efficient auxiliary transporter tool for carrying Ad into cells. Although (Ac-YGGRGDTP$_\beta$A)$_2$K-PEG-$_\beta$AC-SHS could not be purified by HPLC owing to its instability in water, quality of this tool when constructed in situ was still sufficient to modify Ad. Various active esters of 6-maleimidohexanoic acid are presently being examined in order to obtain a stable 6-[(Ac-YGGRGDTP$_\beta$A)$_2$K-PEG-$_\beta$AC-succinimido]hexanoic acid active ester in water.

Recently, Ogawara et al.[12] reported a procedure that modified Ad in two steps, using PEG and cyclic RGD peptide. These authors prepared PEG-Ad and then combined cyclic RGD peptide (Ansynth, Netherlands) with the pegylated Ad. Our own future studies will investigate peptide-PEG transporters, which can modify Ad in just one step.

References and notes

1. This paper was reported at The 123rd Annual Meeting of The Pharmaceutical Society of Japan, Nagasaki, Japan, Mar 27–29, 2003.
2. (a) Crystal, R. G. *Science* **1955**, *270*, 404–4010; (b) Wilson, J. M. *New Engl. J. Med.* **1996**, *334*, 1185.
3. (a) Bergelson, J. M.; Cunningham, J. A.; Droguett, G.; Kurt-Jones, E. A.; Krithivas, A.; Hong, J. S.; Horwitz, M. S.; Crowell, R. L.; Finberg, R. W. *Science* **1997**, *275*, 1320; (b) Bewley, M. C.; Springer, K.; Zhang, Y. B.; Freimuth, P.; Flanagan, J. M. *Science* **1999**, *286*, 1579.
4. (a) Wickham, T. J.; Mathias, P.; Cheresh, D. A.; Nemerow, G. R. *Cell* **1993**, *73*, 309–319; (b) Bai, M.; Harfe, B.; Freimuth, P. *J. Virol.* **1993**, *67*, 5198.
5. Van Ginkel, F. W.; Liu, C.-G.; Simecka, J. W.; Dong, J.-Y.; Greenway, T.; Frizzell, R. A.; Kiyono, H.; McGhee, J. R.; Pascual, D. W. *Hum. Gene Ther.* **1995**, *6*, 895.
6. (a) Romanczuk, H.; Galer, C. D.; Zabner, J.; Barsomian, G.; Wadsworth, S. C.; O'Riordan, C. R. *Hum. Gene Ther.* **1999**, *1*, 2615; (b) Croyle, M. A.; Chirmule, N.; Zhang, Y.; Wilson, J. M. *J. Viol.* **2001**, *75*, 4792; (c) Croyle, M. A.; Chirmule, N.; Zhang, Y.; Wilson, J. M. *Hum. Gene Ther.* **2002**, *10*, 1887.
7. Eto, Y.; Gao, J.; Sekiguchi, F.; Kurachi, S.; Katayama, K.; Mizuguchi, H.; Hayakawa, T.; Tsutsumi, Y.; Mayumi, T.; Nakagawa, S. *Biol. Pharm. Bull.* **2004**, *27*, 936.
8. Erbacher, P.; Remy, J. S.; Behr, J. P. *Gene Ther.* **1999**, *6*, 138.
9. (a) Hashida, S.; Imagawa, M.; Inoue, S.; Ruan, K. H.; Ishikawa, E. *J. Appl. Biochem.* **1984**, *6*, 53; (b) Fargeas, C.; Hommel, M.; Maingon, R.; Dourado, C.; Monsigny, M.; Mayer, R. *J. Clin. Microbiol.* **1996**, *2*, 241.
10. (a) Rink, H. *Tetrahedron Lett.* **1987**, *28*, 3787; (b) Bernatowicz, M. S.; Daniels, S. B.; Köster, H. *Tetrahedron Lett.* **1989**, *30*, 4645.
11. Yield 78 mg (6%, calculated from NH_2 content of the used resin). Amino acid ratios in an acid hydrolysate: Asp, 0.80; Gly, 3.21; Arg, 0.87; Thr, 1.06; Pro, 1.02; Tyr, 0.91; Lys, 0.50. Peptide content calculated from the amino acid analysis, 0.15 mmol/g.
12. Ogawara, K.; Rots, M. G.; Kok, R. J.; Moorlag, H. E.; Loenen, A. V.; Meijer, D. K. F.; Haisma, H. J.; Molema, G. *Human Gene Ther.* **2004**, *15*, 433.

Available online at www.sciencedirect.com
SCIENCE DIRECT®
Biochemical and Biophysical Research Communications 328 (2005) 1043–1050
BBRC
www.elsevier.com/locate/ybbrc

A single intratumoral injection of a fiber-mutant adenoviral vector encoding interleukin 12 induces remarkable anti-tumor and anti-metastatic activity in mice with Meth-A fibrosarcoma☆

Jian-Qing Gao[a,b], Toshiki Sugita[a], Naoko Kanagawa[a], Keisuke Iida[a], Yusuke Eto[a], Yoshiaki Motomura[a], Hiroyuki Mizuguchi[c], Yasuo Tsutsumi[c], Takao Hayakawa[d], Tadanori Mayumi[e], Shinsaku Nakagawa[a,*]

[a] *Department of Biopharmaceutics, Graduate School of Pharmaceutical Sciences, Osaka University, 1-6 Yamadaoka, Suita, Osaka 565-0871, Japan*
[b] *Department of Pharmaceutics, College of Pharmaceutical Sciences, Zhejiang University, 353 Yan-an Road, Hangzhou, Zhejiang 310031, PR China*
[c] *National Institute of Health Sciences, Osaka Branch Fundamental Research Laboratories for Development of Medicine, 1-1-43 Hoenzaka, Chuo-ku, Osaka 540-0006, Japan*
[d] *National Institute of Health Sciences, 1-18-1 Kamiyoga, Setagaya-ku, Tokyo 158-8501, Japan*
[e] *Department of Cell Therapeutics, Graduate School of Pharmaceutical Sciences, Kobe-gakuin University, 518 Arise, Igawadani, Nishiku, Kobe 651-2180, Japan*

Received 12 January 2005
Available online 25 January 2005

Abstract

Cytokine-encoding viral vectors are considered to be promising in cancer gene immunotherapy. Interleukin 12 (IL-12) has been used widely for anti-tumor treatment, but the administration route and tumor characteristics strongly influence therapeutic efficiency. Meth-A fibrosarcoma has been demonstrated to be insensitive to IL-12 treatment via systemic administration. In the present study, we developed an IL-12-encoding fiber-mutant adenoviral vector (AdRGD-IL-12) that showed enhanced gene transfection efficiency in Meth-A tumor cells, and the production of IL-12 p70 in the culture supernatant from transfected cells was confirmed by ELISA. In therapeutic experiments, a single low-dose (2×10^7 plaque-forming units) intratumoral injection of AdRGD-IL-12 elicited pronounced anti-tumor activity and notably prolonged the survival of Meth-A fibrosarcoma-bearing mice. Immunohistochemical staining revealed that the IL-12 vector induced the accumulation of T cells in tumor tissue. Furthermore, intratumoral administration of the vector induced an anti-metastasis effect as well as long-term specific immunity against syngeneic tumor challenge.

Keywords: Interleukin 12; Meth-A fibrosarcoma; Recombinant adenoviral vector; Anti-tumor; Anti-metastasis; Intratumoral administration; IL-12 insensitive

The immunostimulating cytokine interleukin 12 (IL-12), a heterodimeric protein composed of two disulfide-linked subunits, is secreted by dendritic cells as well as macrophages and is a key mediator of immunity [1,2]. A variety of studies have focused on the use of IL-12 in cancer therapy and, in these experiments, IL-12 has exhibited potent anti-tumor activity in a number of tumor models [3–5]. IL-12 acts on T and natural killer (NK) cells by enhancing the generation and activity of cytotoxic T lymphocytes and inducing the proliferation and production of cytokines, especially interferon-γ [6]. In addition, IL-12 inhibits

☆ *Abbreviations:* Ad vector, adenoviral vector; AdRGD, RGD fiber-mutant Ad vector; FBS, fetal bovine serum; IL-12, interleukin 12; MOI, multiplicity of infection; PBS, phosphate-buffered saline; PFU, plaque-forming units; $TCID_{50}$, tissue culture infectious $dose_{50}$.

* Corresponding author. Fax: +81 6 6879 8179.
E-mail address: nakagawa@phs.osaka-u.ac.jp (S. Nakagawa).

0006-291X/$ - see front matter © 2005 Elsevier Inc. All rights reserved.
doi:10.1016/j.bbrc.2005.01.061

tumor angiogenesis mainly through IFN-γ-dependent production of the chemokine interferon-inducible protein-10 (IP-10) [7].

Several mechanisms of the anti-tumor activity of IL-12 have been identified, and each contributes differently to the overall therapeutic outcome in a given tumor model [8–10]. Further, some tumor models, such as Meth-A and MCH-1A1 cells, are resistant to treatment with systemically administered IL-12 [11,12]. For example, intraperitoneal administration of murine recombinant IL-12 failed to inhibit the growth of Meth-A fibrosarcoma, even at a dosage of 500 ng daily for 3 days [11]. Compared with so-called IL-12-sensitive tumor cells such as OV-HM ovarian carcinoma and CSA1M fibrosarcoma, which both exhibited notable tumor regression after IL-12-stimulated T-cell infiltration into tumor tissues, Meth-A and MCH-1-A1 tumors lacked similar accumulation of immune cells [12]. Furthermore, otherwise exciting tumor regression results from preclinical studies were moderated by the severe adverse effects that occurred after systemic administration of IL-12 in murine models [13]. The clinical development of IL-12 as a single recombinant protein for systemic therapy has been tempered by pronounced toxicity and disappointing anti-tumor effects [14].

Intratumoral administration of IL-12 may offer several potential advantages over systemic dosing, such as delivery of the gene directly to the tissue of interest and avoidance of the drawbacks of systemic delivery, including the induction of toxicity, acute allergic reactions, and other adverse effects due to the encoded gene [15]. The results of one clinical trial suggest that intratumoral injection of $\leqslant 3 \times 10^{12}$ viral particles of an IL-12-encoding adenoviral vector in patients with advanced gastrointestinal malignancies is feasible and well tolerated [16].

In the present study, we constructed a recombinant adenovirus (Ad) vector that encoded IL-12 (AdRGD-IL-12); the gene transfection efficiency of AdRGD-IL-12 was higher than that of a conventional Ad vector. We also investigated the feasibility of using a single intratumoral injection of AdRGD-IL-12 to provide effective cancer treatment for primary and metastatic Meth-A fibrosarcoma. Furthermore, immunostaining was used to measure the postinjection infiltration of immune cells into tumor tissue.

Materials and methods

Cell lines and animals. Meth-A fibrosarcoma cells (BALB/c origin) were kindly provided by Dr. Hiromi Fujiwara (School of Medicine, Osaka University, Osaka, Japan) and were maintained by intraperitoneal passage in syngeneic BALB/c mice. Human embryonic kidney (HEK) 293 cells were cultured in DMEM supplemented with 10% FBS. BALB/c female mice were obtained from SLC (Hamamatsu, Japan) and used at 6–8 weeks of age. All of the experimental procedures were performed in accordance with the Osaka University guidelines for the welfare of animals in studies of experimental neoplasia.

Vector construction. The replication-deficient AdRGD vector was based on the adenovirus serotype 5 backbone with deletions of E1/E3 region. The RGD sequence for αv-integrin targeting was inserted into the HI loop of the fiber knob by using a two-step method, as previously described [17]. AdRGD-Luc, which is identical to the AdRGD-IL-12 vectors but with the substitution of the luciferase gene expression cassette for the cytokine, was used as negative control vector in the present study. The replication-deficient AdRGD-IL-12, which carries the murine IL-12 gene derived from mIL-12 BIA/pBluescript II KS(−) [18] (kindly provided by Prof. Hiroshi Yamamoto, Graduate School of Pharmaceutical Sciences, Osaka University, Suita, Japan), was constructed by an improved in vitro ligation method using pAdHM15-RGD [19,20]. The expression cassette, which was designed to be transcribed in order from the IL-12 p35 cDNA through the internal ribosome entry site sequence to the IL-12 p40 cDNA under the control of the cytomegalovirus promoter, was inserted into the E1-deletion region of the E1/E3-deleted Ad vector (Fig. 1). All vectors were propagated in HEK293 cells, purified by two rounds of CsCl gradient centrifugation, dialyzed with phosphate-buffered saline (PBS) containing 10% glycerol, and stored at −80 °C. The number of viral particles in vector stock was determined spectrophotometrically by the method of Maizel et al. [21]. Titers (tissue culture infectious $dose_{50}$; $TCID_{50}$) of infective AdRGD particles were evaluated by the end-point dilution method using HEK293 cells and expressed as plaque-forming units (PFU).

Gene expression by AdRGD-Luc or conventional Ad-Luc in Meth-A cells. Meth-A cells were plated in 96-well plates at a density of 2×10^3 cells/well and incubated with Ad-Luc or AdRGD-Luc at concentrations of 1250, 2500, 5000, or 10,000 viral particles/cell for 1.5 h. Cells were then washed with PBS and cultured for an additional 48 h. Subsequently, the cells were washed, collected, and lysed with Luciferase Cell Culture Lysis buffer (Promega, USA), and their luciferase activity was measured by the Luciferase Assay System (Promega,

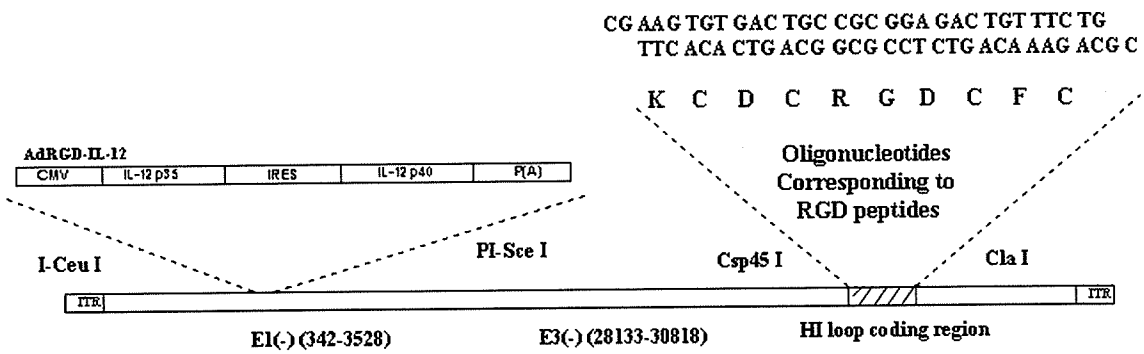

Fig. 1. Construction of IL-12 encoding fiber-mutant adenoviral vector.

USA) and Microlumat Plus LB96 (Perkin-Elmer) according to the manufacturer's instructions.

Analysis of gene transduction of AdRGD-IL-12 in vitro. Meth-A cells were plated in six-well plates at a density of 5×10^5 cells/well and transfected with AdRGD-IL-12 for 24 h at various multiplicities of infection (MOIs) in 2 ml RPMI 1640 medium containing 10% FBS. After three washes of the transfected cells with PBS, a 1.5-ml aliquot of culture medium was added to each well. The supernatants were collected after 24 h, and the amount of IL-12 p70 in each sample was measured with a murine IL-12 p70 ELISA kit (Biosource International, Camarillo, CA, USA) according to the manufacturer's instructions.

Tumor inoculation and intratumoral administration of vectors in animal experiments. Meth-A cells were inoculated intradermally into the flanks of BALB/c mice at 2×10^6 cells/mouse. After 7 days, established tumors (diameter, 9–10 mm) were injected with each vector at 2×10^7 plaque-forming units (PFU) in 50 μl PBS. Tumor size (length and width in mm) was measured twice weekly; animals were euthanized when either of the two parameters exceeded 20 mm. At 3 months after complete regression of the primary tumors, mice were challenged with freshly isolated Meth-A tumor cells or CT26 cells by intradermal injection of 1×10^6 cells into the flank.

Immunohistochemical staining. T-cell infiltration into the Meth-A tumors after intratumoral injection of AdRGD-IL-12 was determined by immunohistochemical analysis. Tumor-bearing mice were euthanized 6 days after administration of AdRGD-IL-12 or the control vector. The tumor nodules were harvested, embedded in OCT compound (Sakura, Torrance, CA, USA), and stored at −80 °C. Frozen thin (6-μm) sections of the nodules were fixed in 4% paraformaldehyde solution, washed with Tris-buffered saline (TBS), and incubated in methanol containing 0.3% hydrogen peroxide for 30 min at room temperature to block endogenous peroxidase activity. The sections were incubated with the optimal dilution of the primary antibody—either rabbit anti-human CD3 antibody (DakoCytomation) or normal rabbit IgG (Santa Cruz Biotechnology)—for 60 min at room temperature. Bound primary antibody was detected after incubation with the secondary antibody from the EnVision+ System (DakoCytomation) for 30 min, followed by a 15-min wash in TBS. The sections were stained with DAB (DakoCytomation) and finally counterstained with hematoxylin (DakoCytomation). We randomly selected six fields from different tumor sections and counted the immunostained cells under a light microscope at 400× magnification.

Experiments on metastatic tumor. We intradermally inoculated mice with 2×10^6 Meth-A cells as described earlier and, 5 days later, injected 8×10^4 cells intravenously. Two days after the intravenous injection, intratumoral injection of AdRGD-IL-12 (2×10^7 PFU) was carried out. The size of the primary tumor was measured twice weekly, and the lungs were harvested 2 weeks after the intravenous injection. The lungs were weighed, sectioned for histology, and stained with hematoxylin and eosin. Metastases in the lungs were identified under a light microscope.

Statistical analysis. Student's t test was used for statistical comparison when applicable. Differences were considered statistically significant at $P < 0.05$.

Results

Meth-A tumor cells transfected with the fiber-mutant adenoviral vector induce higher luciferase gene expression than do those induced with the conventional vector

To evaluate the gene transfection efficiency of the fiber-mutant Ad vector developed for this study, Meth-A cells were transfected with either the conventional Ad-Luc vector or the fiber-mutant AdRGD-Luc vector at various MOIs and the luciferase activity was measured. The luciferase gene expression due to transfection of the fiber-mutant vector was much higher than that from the conventional vector (Fig. 2). For example, at 5000 and 10,000 viral particles/cell, 16.8-fold and 15.7-fold greater gene expression, respectively, was obtained in response to AdRGD-Luc than to Ad-Luc. These results show that insertion of the RGD peptide into the viral fiber enhanced the transfection efficiency of the Ad vector into Meth-A cells.

Expression of IL-12 p70 in Meth-A cells via transfection of AdRGD-IL-12

The IL-12-encoding fiber-mutant adenoviral vector AdRGD-IL-12 was developed as shown in Fig. 1. To confirm the biological activity of AdRGD-IL-12, we used an ELISA to measure the amount of IL-12 in the

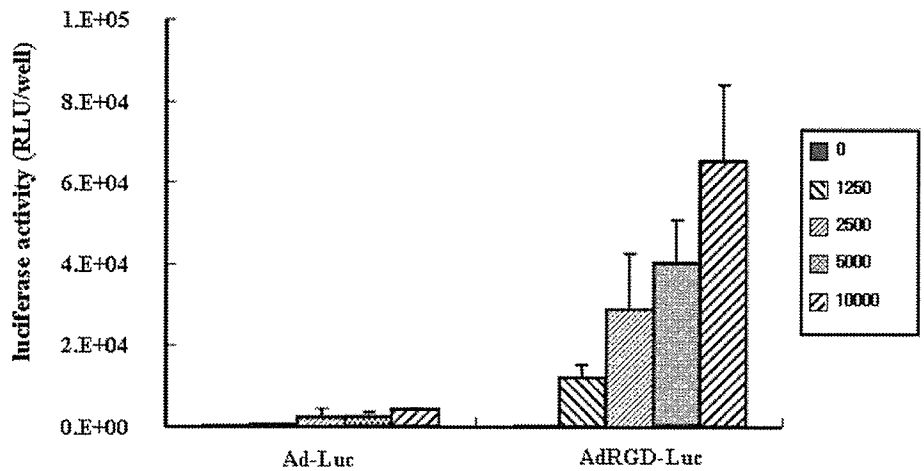

Fig. 2. Gene expression by AdRGD-Luc or conventional Ad-Luc in Meth-A cells. Meth-A cells (2×10^3/well) in 96-well plates were treated with Ad-Luc or AdRGD-Luc at the indicated numbers of viral particles/cell for 1.5 h. Cells were washed and cultured for an additional 48 h. Subsequently, the cells were washed, collected, and their luciferase activity was measured. Data are presented as means ± SE of relative light units (RLUs)/well from three experiments.

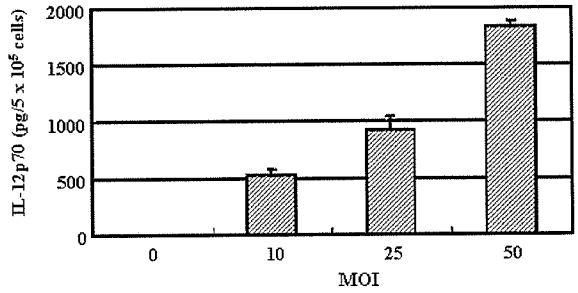

Fig. 3. Production of IL-12 p70 from Meth-A cells transfected with AdRGD-IL-12. We transfected 5×10^5 Meth-A cells with AdRGD-IL-12 for 24 h at the indicated multiplicities of infection (MOIs). Then the cells were cultured for a further 24 h with fresh medium. The supernatants were collected and the IL-12 p70 level was measured by ELISA.

supernatants of transfectants. Meth-A cells transfected with AdRGD-IL-12 showed dose-dependent concentrations of IL-12 p70 in the supernatants. In contrast, no detectable IL-12 p70 was present in the culture media of cells that had not been transfected (Fig. 3).

Anti-tumor activity and long-term specific immune response are induced by intratumoral injection of AdRGD-IL-12

The growth of Meth-A tumors was suppressed dramatically, and complete regression occurred in about 70% of the tumor-bearing mice after a single intratumoral injection of 2×10^7 PFU of AdRGD-IL-12. In contrast, the AdRGD-Luc group showed no apparent anti-tumor effect (Fig. 4A). In addition, the relative survival rates further demonstrated prolonged survival after treatment with IL-12 (Fig. 4B). In the rechallenge

Table 1
Specific long-term anti-tumor immune response to IL-12 treatment

Groups	Challenging cell	Tumor rejected mice/challenged mice
Intact mice	Meth-A[a]	0/5
Meth-A rejected[c]	Meth-A[a]	5/5
Meth-A rejected[d]	CT26[b]	0/3

[a] Challenged with 1×10^6 cells.
[b] Challenged with 3×10^5 cells.
[c] Meth-A cured; Meth-A rechallenged.
[d] Meth-A cured; CT26 rechallenged.

experiment, mice showing complete regression were reinoculated intradermally with Meth-A or CT26 cells 90 days after the initial injection of tumor cells. All of the mice challenged with Meth-A cells remained tumor-free for at least 2 months (Table 1). In contrast, 100% of the mice challenged with CT26 developed palpable tumors within 2 weeks. These results indicate the generation of specific immunity against Meth-A tumor cells in those mice that rejected Meth-A upon treatment with IL-12.

Intratumoral administration of AdRGD-IL-12 induces the infiltration of T cells into Meth-A tumors

To investigate the anti-tumor mechanism of AdRGD-IL-12, tumor tissues were subjected to immunohistochemical staining for CD3 six days after treatment with AdRGD-IL-12 or AdRGD-Luc. Tissues from mice that received AdRGD-IL-12 demonstrated significantly increased accumulation of $CD3^+$ T cells compared with animals injected with either AdRGD-Luc or PBS (Fig. 5).

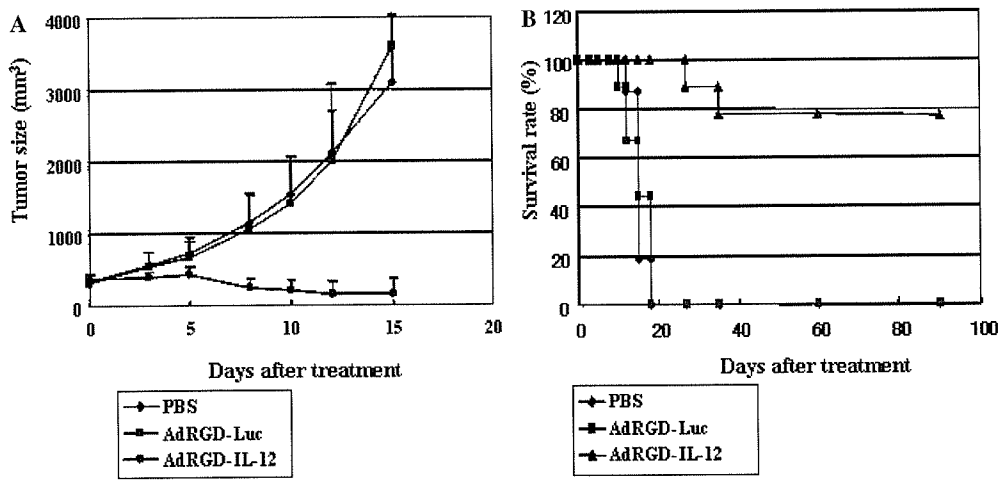

Fig. 4. Growth in BALB/c mice of established Meth-A tumor cells injected intratumorally with IL-12-encoding adenoviral vector. Mice were inoculated intradermally in the flank with 2×10^6 Meth-A cells (100 μl in RPMI 1640). They were then intratumorally injected with 2×10^7 PFU AdRGD-IL-12, AdRGD-Luc, or PBS. Tumor volume was calculated after measuring the length and width of tumors at the indicated time points, and data are expressed as means ± SE of results obtained from at least eight mice. Animals were euthanized when either the length or width of the tumor exceeded 20 mm. (A) Average tumor size. (B) Survival rate (%) of mice.

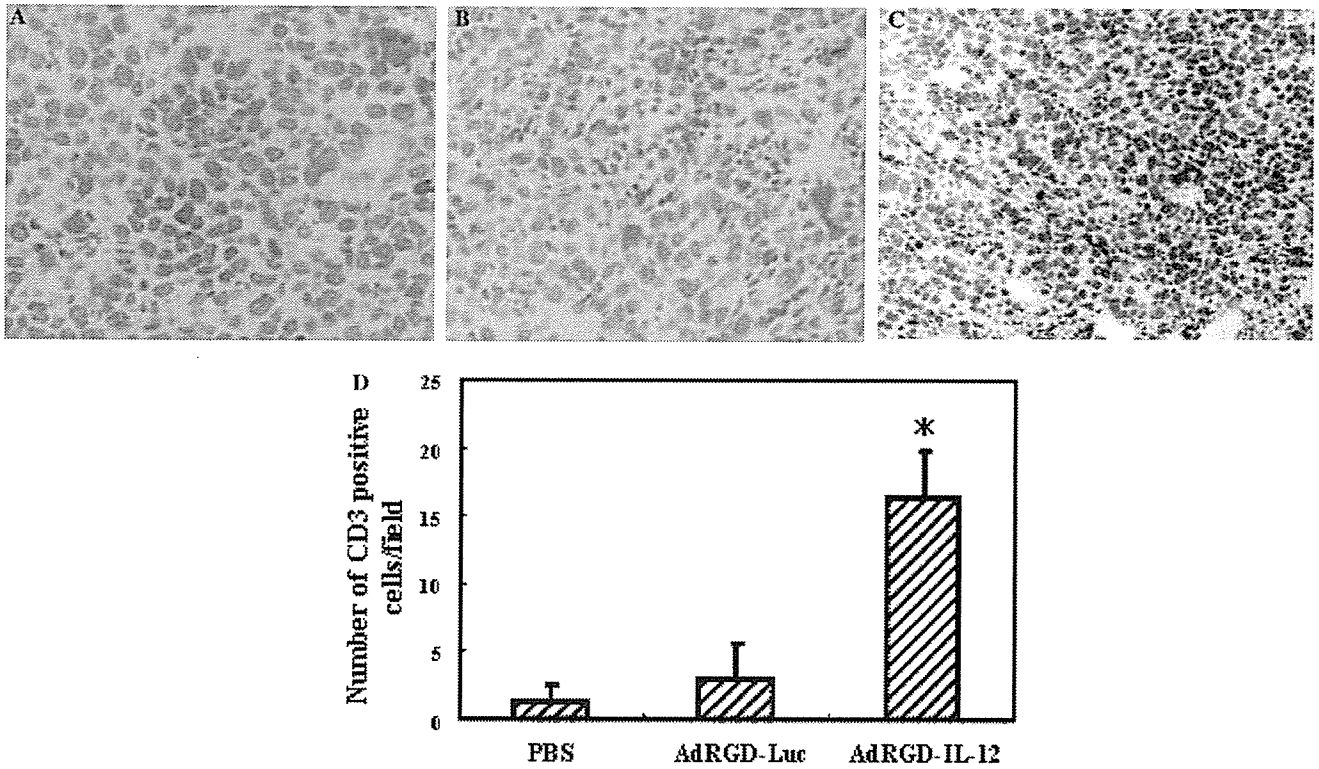

Fig. 5. Intratumoral injection of AdRGD-IL-12 induced the infiltration of $CD3^+$ T cells into Meth-A tumors. Representative views of tumor nodules from mice, harvested 6 days after intratumoral injection of the indicated vectors and controls, and stained for CD3. (A) PBS, (B) AdRGD-Luc, (C) AdRGD-IL-12. The photographs were obtained under light microscopy at 400× magnification. (D) Six fields from different tumor sections were randomly selected and positive cell number infiltrated into tumor tissue was counted. $*P < 0.05$ with Student's t test in groups between treated with AdRGD-IL-12 and AdRGD-Luc or PBS.

Anti-metastatic activity is induced by intratumoral injection of AdRGD-IL-12

We then sought to evaluate whether intratumoral injection of AdRGD-IL-12 would induce anti-tumor effects against both the primary and metastatic tumors. Our results showed that single intratumoral injection of AdRGD-IL-12 induced pronounced anti-metastasis activity (Figs. 6A and B) while maintaining tumor-suppressive activity toward the primary tumor, similar to

A

Group	Metastasis-free mice/mice in group	Occurrence of Metastasis (%)
PBS	0/8	100%
AdRGD-Luc	1/9	89%
AdRGD-IL-12	8/9	11%

B

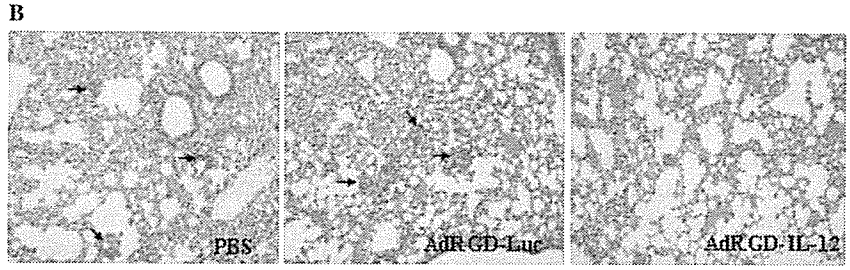

Fig. 6. Anti-metastatic activity due to intratumoral injection of AdRGD-IL-12 into Meth-A fibrosarcoma. (A) Incidence of metastasis in each group. (B) Photomicrographs of lung tissue harvested 2 weeks after treatment and stained with hematoxylin and eosin. The photographs were obtained under light microscopy at 10× magnification. The arrows indicate micrometastasizing tumor.

that shown in Fig. 4 (data not shown). Compared with the control group treated with AdRGD-Luc, in which about 90% of the mice had readily discernable lung metastasis, only one of nine animals treated with AdRGD-IL-12 demonstrated metastasis.

Discussion

Viral vector-encoded chemokines and cytokines are used widely in cancer gene therapy [22,23]. IL-12 has demonstrated remarkable anti-tumor activity when used directly as a recombinant protein or after various viral and non-viral vectors have been used to transfer its genes [24–26]. The development of an efficient vector is pivotal for gene therapy. Because of its high transfection efficiency and because it can transfect both dividing and quiescent cells, Ad vectors are used widely in gene therapy protocols: about 26% of gene therapy clinical trials use Ad vectors as gene carriers [27,28]. However, the lack of Coxsackie adenovirus receptor (CAR), which is an important receptor for conventional Ad vector infection, in many types of malignant cells impairs the tranfection efficiency with Ad vector [29]. Meth-A fibrosarcoma has been confirmed by RT-PCR to be deficient in expression of CAR but with expression of integrin (data not shown). Our previous reports have also shown that insertion of the RGD peptide into the fiber sequences of Ad vectors induces enhanced gene transfection in CT26 and A2058 cells [30,31]. The results of our present study also demonstrate that the fiber-mutant Ad vector induced enhanced expression of the encoded luciferase gene in Meth-A fibrosarcoma cells compared with the expression due to conventional vector (Fig. 2). Furthermore, we confirmed the presence of IL-12 p70 in the supernatant of Meth-A cells transfected with AdRGD-IL-12 (Fig. 3).

Systemic administration of recombinant IL-12 at high doses induces adverse effects associated with high systemic peak concentrations [32,33]. Therefore, gene transfer methods are designed to confine IL-12 production to the tumor environment, thereby preventing systemic toxicity. Tumor cells, dendritic cells, and autologous fibroblasts have been transfected with recombinant adenoviruses or retroviruses to secrete IL-12 locally and have shown favorable efficacy and safety profiles [34,35]. Several groups have shown that intratumoral injection of an Ad vector encoding IL-12 efficiently eradicates experimental gastrointestinal cancer [36,37]. Disadvantages of direct topical administration include tissue damage, and some tumor sites may be inaccessible even to computed tomography-guided percutaneous injection and radiographically directed delivery [38]. However, these limitations favor those types of gene therapy that do not require all tumor cells or tumor masses that express the gene.

Meth-A has shown that it is an IL-12-insensitive tumor cell, in that established tumors could not be treated efficiently via systemic administration of IL-12 and could not even be suppressed effectively (i.e., only 42.5% of mice rejected the tumor) after transfection of an IL-12-containing retroviral vector [12,39]. In our present study, however, a single intratumoral injection of a relatively low dose of AdRGD-IL-12 (2×10^7 PFU) elicited strong anti-tumor activity against established tumors (i.e., diameter of about 10 mm at the beginning of treatment; Fig. 4A). Treatment induced complete tumor regression in about 70% of tumor-bearing mice, and the growth rates of the remaining tumors seem to have been retarded (individual data not shown). Treatment also prolonged the survival of the mice significantly compared with that of the group injected with AdRGD-Luc, a control vector (Fig. 4B). Meanwhile, no detectable IL-12 and IFN-γ existed in the sera after treatment (data not shown)—findings that are consistent with those other reports [40]. Furthermore, intratumoral injection of AdRGD-IL-12 induced a profound long-term specific anti-tumor immunity in mice with complete regression of the initial Meth-A lesion (Table 1).

Studies have shown that IL-12 elicits tumor regression after induction of T-cell migration to tumor sites [41]. The failure of IL-12 therapy in Meth-A via systemic administration is thought to be due to the inability to recruit immune cell migration into tumor cells, and further investigation has indicated a key role of the peritumoral stroma/stromal vasculature in the acceptance of the tumor-infiltrating T cells that are a prerequisite for IL-12-induced tumor regression [12]. Our results similarly demonstrated the accumulation and uniform distribution of $CD3^+$ T cells in the tumor after intratumoral injection, thus supporting the notion that the pronounced anti-tumor effect is related to immune cell infiltration (Fig. 5). However, it remains unclear why intratumoral injection but not systemic administration induces immune cell accumulation in tumor tissue.

We also evaluated the anti-metastasis activity associated with a single intratumoral injection of AdRGD-IL-12. Metastasis is a challenge for cancer treatment, especially because almost all immunotherapy performed in the clinical setting is adjuvant treatment given after surgical reduction of the primary tumor mass for controlling recurrence and metastasis. Interestingly, the single intratumoral injection of AdRGD-IL-12 did induce anti-tumor activity toward disseminated tumors in the lung: histopathology confirmed the complete absence of metastatic tumors in eight of the nine mice tested (and only sporadic residual tumor in the remaining animal). In contrast, all mice that received intratumoral injection of the control vector developed metastases, suggesting that local expression of IL-12 also stimulates the systemic immune response to subsequently affect distant malignant cells.

All the results of our present study indicate that a single intratumoral injection of an IL-12-encoding fiber-mutant Ad vector induces T-cell infiltration into stroma-deficient Meth-A fibrosarcoma and is effective in the treatment of, and protection against challenge with, syngeneic tumors. Our results also suggest that a single intratumoral administration of AdRGD-IL-12 can induce a curative immune response in the face of a micrometastasizing tumor.

Acknowledgments

This study was supported by grants from the Ministry of Health, Labor, and Welfare of Japan and by Grants-in-Aid for Scientific Research on Priority Areas from the Ministry of Education, Culture, Sports, Science and Technology of Japan.

References

[1] M.J. Brunda, Interleukin-12, J. Leukoc. Biol. 55 (1994) 280–288.
[2] G. Trinchieri, Interleukin-12: A proinflammatory cytokine with immunoregulatory functions that bridge innate resistance and antigen-specific adaptive immunity, Annu. Rev. Immunol. 13 (1995) 251–276.
[3] M.P. Colombo, G. Trinchieri, Interleukin-12 in anti-tumor immunity and immunotherapy, Cytokine Growth Factor Rev. 13 (2002) 155–168.
[4] A. Maheshwari, S. Han, R.I. Mahato, S.W. Kim, Biodegradable polymer-based interleukin-12 gene delivery: Role of induced cytokines, tumor infiltrating cells and nitric oxide in anti-tumor activity, Gene Ther. 9 (2002) 1075–1084.
[5] J.W. Yockman, A. Maheshwari, S.O. Han, S.W. Kim, Tumor regression by repeated intratumoral delivery of water soluble lipopolymers/p2CMVmIL-12 complexes, J. Control Release 87 (2003) 177–186.
[6] C.L. Nastala, H.D. Edington, T.G. McKinney, H. Tahara, M.A. Nalesnik, M.J. Brunda, M.K. Gately, S.F. Wolf, R.D. Schreiber, W.J. Storkus, Recombinant IL-12 administration induces tumor regression in association with IFN-γ production, J. Immunol. 153 (1994) 1697–1706.
[7] W.G. Yu, M. Ogawa, J. Mu, K. Umehara, T. Tsujimura, H. Fujiwara, T. Hamaoka, IL-12-induced tumor regression correlates with in situ activity of IFN-gamma produced by tumor-infiltrating cells and its secondary induction of anti-tumor pathways, J. Leukoc. Biol. 62 (1997) 450–457.
[8] J. Cui, T. Shin, T. Kawano, H. Sato, E. Kondo, I. Toura, Y. Kaneko, H. Koseki, M. Kanno, M. Taniguchi, Requirement for valpha 14 NKT cells in IL-12-mediated rejection of tumors, Science 278 (1997) 1623–1626.
[9] M. Iwasaki, W.G. Yu, Y. Uekusa, C. Nakajima, Y.F. Yang, P. Gao, R. Wijesuriya, H. Fujiwara, T. Hamaoka, Differential IL-12 responsiveness of T cells but not of NK cells from tumor-bearing mice in IL-12-responsive versus -unresponsive tumor models, Int. Immunol. 12 (2000) 701–709.
[10] M.J. Smyth, M. Taniguchi, S.E. Street, The anti-tumor activity of IL-12: Mechanisms of innate immunity that are model and dose dependent, J. Immunol. 165 (2000) 2665–2670.
[11] H. Fujiwara, T. Hamaoka, Antitumor and antimetastatic effects of interleukin 12, Cancer Chemother. Pharmacol. 38 (1996) S22–S26.
[12] M. Ogawa, K. Umehara, W.G. Yu, Y. Uekusa, C. Nakajima, T. Tsujimura, T. Kubo, H. Fujiwara, T. Hamaoka, A critical role for a peritumoral stromal reaction in the induction of T-cell migration responsible for interleukin-12-induced tumor regression, Cancer Res. 59 (1999) 1531–1538.
[13] M.J. Brunda, L. Luistro, R.R. Warrier, R.B. Wright, B.R. Hubbard, M. Murphy, S.F. Wolf, M.K. Gately, Antitumor and antimetastasis activity of interleukin 12 against murine tumors, J. Exp. Med. 178 (1993) 1223–1230.
[14] J. Cohen, IL-12 deaths: Explanation and a puzzle, Science 270 (1995) 908.
[15] E.T. Akporiaye, E. Hersh, Clinical aspects of intratumoral gene therapy, Curr. Opin. Mol. Ther. 1 (1999) 443–453.
[16] B. Sangro, G. Mazzolini, J. Ruiz, M. Herraiz, J. Quiroga, I. Herrero, A. Benito, J. Larrache, J. Pueyo, J.C. Subtil, C. Olague, J. Sola, B. Sadaba, C. Lacasa, I. Melero, C. Qian, J. Prieto, Phase 1 trial of intratumoral injection of an adenovirus encoding interleukin-12 for advanced digestive tumors, J. Clin. Oncol. 22 (2004) 1389–1397.
[17] H. Mizuguchi, N. Koizumi, T. Hosono, N. Utoguchi, Y. Watanabe, M.A. Kay, T. Hayakawa, A simplified system for constructing recombinant adenoviral vectors containing heterologous peptides in the HI loop of their fiber knob, Gene Ther. 8 (2001) 730–735.
[18] S. Obana, H. Miyazawa, E. Hara, T. Tamura, H. Nariuchi, M. Takata, S. Fujimoto, H. Yamamoto, Induction of anti-tumor immunity by mouse tumor cells transfected with mouse interleukin-12 gene, Jpn. J. Med. Sci. Biol. 48 (1995) 221–236.
[19] H. Mizuguchi, M.A. Kay, Efficient construction of a recombinant adenovirus vector by an improved in vitro ligation method, Hum. Gene Ther. 9 (1998) 2577–2583.
[20] H. Mizuguchi, M.A. Kay, A simple method for constructing E1- and E1/E4-deleted recombinant adenoviral vectors, Hum. Gene Ther. 10 (1999) 2013–2017.
[21] J.V. Maizel Jr., D.O. White, M.D. Scharff, The polypeptides of adenovirus. I. Evidence for multiple protein components in the virion and a comparison of types 2, 7A, and 12, Virology 36 (1968) 115–125.
[22] J.Q. Gao, Y. Tsuda, K. Katayama, T. Nakayama, Y. Hatanaka, Y. Tani, H. Mizuguchi, T. Hayakawa, O. Yoshie, Y. Tsutsumi, T. Mayumi, S. Nakagawa, Anti-tumor effect by interleukin-11 receptor alpha-locus chemokine/CCL27, introduced into tumor cells through a recombinant adenovirus vector, Cancer Res. 63 (2003) 4420–4425.
[23] R. Dummer, J.C. Hassel, F. Fellenberg, S. Eichmuller, T. Maier, P. Slod, B. Acres, P. Bleuzen, V. Bataille, P. Squiban, G. Burg, M. Urosevic, Adenovirus-mediated intralesional interferon-gamma gene transfer induces tumor regressions in cutaneous lymphomas, Blood 104 (2004) 1631–1638.
[24] A.M. Orengo, E.D. Carlo, A. Comes, M. Fabbi, T. Piazza, M. Cilli, P. Musiani, S. Ferrini, Tumor cells engineered with IL-12 and IL-15 genes induce protective antibody responses in nude mice, J. Immunol. 171 (2003) 569–575.
[25] S. Zheng, G. Zeng, D.S. Wilkes, G.E. Reed, R.C. McGarry, J.N. Eble, L. Cheng, Dendritic cells transfected with interleukin-12 and pulsed with tumor extract inhibit growth of murine prostatic carcinoma in vivo, Prostate 55 (2003) 292–298.
[26] S. Gyorffy, K. Palmer, T.J. Podor, M. Hitt, J. Gauldie, Combined treatment of a murine breast cancer model with type 5 adenovirus vectors expressing murine angiostatin and IL-12: A role for combined anti-angiogenesis and immunotherapy, J. Immunol. 166 (2001) 6212–6217.
[27] Wiley website: <http://www.wiley.co.uk/genmed/clinical>.
[28] J.A. St. George, Gene therapy progress and prospects: Adenoviral vectors, Gene Ther. 10 (2003) 1135–1141.
[29] H. Wu, T. Han, J.T. Lam, C.A. Leath, I. Dmitriev, E. Kashentseva, M.N. Barnes, R.D. Alvarez, D.T. Curiel, Preclinical evalu-

ation of a class of infectivity-enhanced adenoviral vectors in ovarian cancer gene therapy, Gene Ther. 11 (2004) 874–878.
[30] Y. Okada, N. Okada, S. Nakagawa, H. Mizuguchi, K. Takahashi, N. Mizuno, T. Fujita, A. Yamamoto, T. Hayakawa, T. Mayumi, Tumor necrosis factor α-gene therapy for an established murine melanoma using RGD (Arg-Gly-Asp) fiber-mutant adenovirus vectors, Jpn. J. Cancer Res. 93 (2002) 436–444.
[31] J.Q. Gao, S. Inoue, Y. Tsukada, K. Katayama, Y. Eto, S. Kurachi, H. Mizuguchi, T. Hayakawa, Y. Tsutsumi, T. Mayumi, S. Nakagawa, High gene expression of mutant adenovirus vector both in vitro and in vivo with the insertion of integrin-targeting peptide into the fiber, Pharmazie 59 (2004) 571–572.
[32] J.P. Leonard, M.L. Sherman, G.L. Fisher, L.J. Buchanan, G. Larsen, M.B. Atkins, J.A. Sosman, J.P. Dutcher, N.J. Vogelzang, J.L. Ryan, Effects of single-dose interleukin-12 exposure on interleukin-12-associated toxicity and interferon-gamma production, Blood 90 (1997) 2541–2548.
[33] S. Sacco, H. Heremans, B. Hchtenacher, W.A. Buurman, Z. Amraoui, M. Goldman, P. Ghezzi, Protective effect of a single interleukin-12 (IL-12) predose against the toxicity of subsequent chronic IL-12 in mice: Role of cytokines and glucocorticoids, Blood 90 (1997) 4473–4479.
[34] C. Lechanteur, M. Moutschen, F. Princen, M. Lopez, E. Franzen, J. Gielen, V. Bours, M.P. Merville, Antitumoral vaccination with granulocyte-macrophage colony-stimulating factor or interleukin-12-expressing DHD/K12 colon adenocarcinoma cells, Cancer Gene Ther. 7 (2000) 676–682.
[35] L. Zitvogel, B. Couderc, J.I. Mayordomo, P.D. Robbins, M.T. Lotze, W.J. Storkus, IL-12-engineered dendritic cells serve as effective tumor vaccine adjuvants in vivo, Ann. N.Y. Acad. Sci. 795 (1996) 284–293.
[36] G. Mazzolini, C. Qian, X. Xie, Y. Sun, J.J. Lasarte, M. Drozdzik, J. Prieto, Regression of colon cancer and induction of antitumor immunity by intratumoral injection of adenovirus expressing interleukin-12, Cancer Gene Ther. 6 (1999) 514–522.
[37] M. Caruso, K. Pham Nguyen, Y.L. Kwong, B. Xu, K.I. Kosai, M. Finegold, S.L. Woo, S.H. Chen, Adenovirus-mediated interleukin-12 gene therapy for metastasis colon carcinoma, Proc. Natl. Acad. Sci. USA 93 (1996) 11302–11306.
[38] E.T. Akporiaye, E. Hersh, Clinical aspects of intratumoral gene therapy, Curr. Opin. Mol. Ther. 1 (1999) 443–453.
[39] H. Fujiwara, N. Yamauchi, Y. Sato, K. Sasaki, M. Takahashi, T. Okamoto, T. Sato, S. Iyama, Y. Koshita, M. Hirayama, H. Yamagishi, Y. Niitsu, Synergistic suppressive effect of double transfection of tumor necrosis factor-α and interleukin 12 genes on tumorigenicity of Meth-A cells, Jpn. J. Cancer Res. 91 (2000) 1296–1302.
[40] Y. Okada, N. Okada, H. Mizuguchi, K. Takahashi, T. Hayakawa, T. Mayumi, N. Mizuno, Optimization of antitumor efficacy and safety of in vivo cytokine gene therapy using RGD fiber-mutant adenovirus vector for preexisting murine melanoma, Biochim. Biophys. Acta 1670 (2004) 172–180.
[41] G. Mazzolini, J. Prieto, I. Melero, Gene therapy of cancer with interleukin 12, Curr. Pharm. Des. 9 (2003) 1981–1991.

ARTICLE

doi:10.1016/j.ymthe.2004.12.017

Eradication of Epstein–Barr Virus Episome and Associated Inhibition of Infected Tumor Cell Growth by Adenovirus Vector-Mediated Transduction of Dominant-Negative EBNA1

Md. Nasimuzzaman,[1,2,*] Masayuki Kuroda,[1,*] Sumitaka Dohno,[1] Takenobu Yamamoto,[1,3] Keiji Iwatsuki,[3] Shigenobu Matsuzaki,[1] Rashel Mohammad,[1] Wakako Kumita,[1] Hiroyuki Mizuguchi,[4] Takao Hayakawa,[5] Hiroyuki Nakamura,[6] Takahiro Taguchi,[7] Hiroshi Wakiguchi,[2] and Shosuke Imai[1,8,†]

[1]*Department of Molecular Microbiology and Infections,* [2]*Department of Pediatrics,* [6]*Department of Environmental Medicine, and* [7]*Department of Neurobiology and Anatomy, Kochi Medical School, Kochi 783-8505, Japan*
[3]*Department of Dermatology, Okayama University Graduate School of Medicine and Dentistry, Okayama 700-8558, Japan*
[4]*Project III, National Institute of Health Sciences, Osaka Branch, Fundamental Research Laboratories for Development of Medicine, 7-6-8 Asagi, Saito, Ibaraki, Osaka 567-0085, Japan,* [5]*Division of Cellular and Gene Therapy Products, National Institute of Health Sciences, Tokyo 158-8501, Japan,* [8]*CREST, Japan Science and Technology Agency, Tokyo, Japan*

**These authors contributed equally to this work.*

[†]*To whom correspondence and reprint requests should be addressed at the Program for Bio-signaling and Infection Control, Department of Molecular Microbiology and Infections, Kochi Medical School, Kohasu, Oko-cho, Nankoku, Kochi 783-8505, Japan. Fax: +81 88 880 2324. E-mail: shoimai@med.kochi-u.ac.jp.*

Available online 30 January 2005

Epstein–Barr virus (EBV) nuclear antigen 1 (EBNA1), a latent viral protein consistently expressed in infected proliferating cells, is essentially required *in trans* to maintain EBV episomes in cells. We constructed a mutant (mt) EBNA1 and examined whether it exerted dominant-negative effects on maintenance of the viral episome thereby leading to abrogation of EBV-infected tumor cell growth. Using lymphocyte and epithelial cell lines converted with neomycin-resistant recombinant EBV (rEBV) as models, adenovirus vector-mediated transduction of mtEBNA1, but not LacZ, brought about rapid and striking reductions in rEBV-derived wild-type EBNA1 levels and viral genomic loads in converted lines of three major viral latencies. This outcome was further validated at the single-cell level by cellular loss of G418 resistance and viral signals *in situ*. The mtEBNA1 transduction significantly impaired growth of naturally EBV-harboring Burkitt lymphoma cells *in vitro* and *in vivo*, largely in association with the eradication of viral episomes. Expression of mtEBNA1 per se caused no detectable cytotoxicity in EBV-uninfected cells. These results indicate that mtEBNA1 can act as a dominant-negative effector that efficiently impedes the EBV-dependent malignant phenotypes in cells regardless of viral latency or tissue origin. The mutant will afford an additional therapeutic strategy specifically targeting EBV-associated malignancies.

Key Words: Epstein–Barr virus, EBNA1 mutant, adenovirus vector, EBV episome eradication, tumor growth inhibition, gene therapy

INTRODUCTION

The Epstein–Barr virus (EBV) is a human gammaherpesvirus that can readily immortalize B lymphocytes *in vitro*, called lymphoblastoid cell lines (LCL). This immortalizing capability is relevant to understanding how EBV acts as the etiological agent of infectious mononucleosis and of often-fatal lymphoproliferative disorders in immunocompromised hosts [1]. EBV is also causally associated with endemic Burkitt lymphoma (BL) and undifferentiated nasopharyngeal carcinoma [1]. Over the past 15 years the array of human cancers potentially related to EBV has increased and now includes Hodgkin disease, subgroups of T or natural killer (NK) cell lymphoma, and gastric carcinoma [1–6].

These EBV-associated malignant diseases are clinically aggressive and often less responsive to conventional

1525-0016/$30.00

therapy, and currently available anti-herpesvirus (lytic-cycle) drugs are ineffective treatments. A unique *in vivo* feature of EBV-associated malignancies is consistent existence (generally monoclonal) and expression of EBV exclusively in tumor cells and not in surrounding normal cells. In addition, considerable evidence has shown that EBV itself and some of its virus-encoded latent genes are actually implicated in certain critical aspects of the oncogenic event in cells [8–18]. These facts, therefore, give enough scope for exploitation of tumor-specific gene therapy that can eliminate EBV itself from malignant cells.

EBV usually persists as a circular extrachromosomal episome in latently infected LCL, or tumor cells (multi-copies per cell in general), in which viral latent genes are expressed in different combinations, generally dependent upon the cell/tumor type [1,7]. The major EBV latent genes include six nuclear antigens (EBNAs 1–6), three latent membrane proteins (LMPs1, 2A, and 2B), two small nonpolyadenylated RNAs (EBERs 1 and 2), and the somewhat complex *Bam*HI-A rightward transcripts (so-called BARTs or CSTs) [7]. Latent EBV infection in dividing cells *in vitro* and *in vivo* is classified into three types according to patterns of latent gene expression: Latencies I, II, and III. A full set of the latent genes is expressed in Latency III, typified by LCL, whereas a restricted set is expressed in Latencies I and II, which are represented by BL and T/NK cell lymphoma, respectively [1].

Of the EBV latent genes, EBNA1 is commonly expressed in EBV-infected proliferating cells irrespective of latency type and tissue origin, although three EBNA transcriptional promoters localized in the *Bam*HI-C, -W, and -Q regions of the EBV genome (Cp, Wp, and Qp, respectively) are differentially utilized [7,19,20]. Biologically, the EBNA1 protein has functional plasticity, as indicated by its role as a transactivator required for viral episome maintenance within cells (replication upon cell division and segregation into daughter cells) and as a transcriptional enhancer for Cp, Wp, and the LMP1/2B promoter via binding to *cis*-acting elements of the latent viral replication origin, *ori*P, in Latency III [21–24]. EBNA1 also participates in the regulation of Qp through binding to a cognate sequence adjacent to Qp in Latencies I and II [25]. Furthermore, EBNA1 may be involved in regulating other genes, transcriptionally or posttranscriptionally, via its protein-binding and/or putative RNA-binding properties or an undefined mechanism(s) [12,26–30]. EBNA1 also elicits immune T cell responses, thereby activating production of some cytokines by T cells, and this, in turn, would promote EBV-infected cell proliferation [31].

Many studies have clarified the precise intramolecular location and functions of some of the domains of the EBNA1 protein [7,22,30,32–34]. Based on domain mapping data, the present study constructed a mutant (mt) EBNA1 gene lacking the most N-terminal half, relative to wild-type (wt) EBNA1, and incorporated it into a conventional replication-incompetent adenovirus serotype 5 vector (Adv5) [35] or its fiber-substituted variant (Adv5/35f) [36]. Utilizing these recombinant adenovirus vectors (Adv's), we examined whether this mtEBNA1 could interrupt the maintenance of EBV episomes in latently infected tumor cells. The results indicated, for the first time, that Adv-mediated transduction of the mtEBNA1 efficiently eradicated viral episomes from cells regardless of viral latency type, tissue origin, or virus strain. Consequently, cellular loss of EBV executed by our mtEBNA1, referred to as dominant-negative (dn) EBNA1, caused remarkable growth inhibition of naturally virus-harboring BL tumor cells. Thus, the dnEBNA1 will provide the basis for a novel, reasonable therapeutic molecule specifically directed against EBV-associated malignancies.

RESULTS

Infection of Cell Lines by Adv

We examined the human cell lines used in this study (Table 1) for efficiency of Adv-mediated gene transfer

TABLE 1: Susceptibility of cell lines to Adv

Cell line	Cell type/EBV latency	%EGFP-positive cells[a] (applied m.o.i. of Adv)						
		1	2	5	10	20	50	70
Akata$^-$/rEBV[b]	B cell/Latency I	45.7	55.1	59.5	67.2	84.0	84.5	85.3
MT-2/rEBV[b]	T cell/Latency II	–	–	85.3	85.3	91.2	94.0	ND
BJAB/rEBV[b]	B cell/Latency III	–	–	48.2	48.2	65.8	83.9	89.8
NU-GC-3/rEBV[b]	Epithelium/Latency I	–	–	74.1	82.5	92.8	94.7	95.8
Mutu I[c]	B cell/Latency I	53.2	59.1	59.8	64.7	63.5	63.9	ND
Akata-EC[c]	B cell/Latency I	34.2	41.5	52.4	60.4	56.2	ND	ND
MRC-5[d]	Fibroblast	–	–	49.3	62.9	78.6	88.9	ND

[a] Flow cytometric analysis data are presented as a percentage of enhanced green fluorescent protein (EGFP)-positive cells over background (control Adv-LacZ inoculation at the same multiplicity of infection (m.o.i.)). Data represent the means of three independent assays performed on each cell line (SD was <6% in all cases). Results obtained using one of the four kinds of Adv's (see Materials and Methods) that produced the highest infectivity are shown here, i.e., Adv5-CV-EGFP for the NU-GC-3/rEBV cell line, Adv5/35f-SV-EGFP for the MRC-5 cell line, and Adv5-SV-EGFP for the other cell lines. Cells were analyzed 3 days after Adv inoculation. –, not tested; ND, not determined due to appearance of significant cytotoxicity caused by Adv-LacZ.
[b] rEBV-converted or -reinfected cell lines.
[c] Naturally occurring BL cell lines.
[d] Human fibroblast.

doi:10.1016/j.ymthe.2004.12.017

using purified Adv's for enhanced green fluorescent protein (EGFP) expression, Adv5-EGFP and Adv5/35f-EGFP (the simian virus 40 early promoter (SVp)-driven and the cytomegalovirus early promoter (CMVp)-driven for each Adv type). Flow cytometric analysis revealed that all cell lines attained maximal EGFP-positive signal of 50–95% for at least one of the four kinds of Adv's (see Materials and Methods) at m.o.i. ranging from 5 to 70 (Table 1). According to these results, we selected an Adv (and promoter) type suitable for each cell line and used it for the following experiments.

Adv-Mediated Expression of mtEBNA1

We checked isolated Adv clones confirmed to be carrying the mtEBNA1 or wtEBNA1 gene construct (Fig. 1) for expression of these proteins by immunoblotting. Representative results of Adv5-CV-DNE1 and Adv5-CV-AKE1 clones (for designation of Adv's, see Materials and Methods) are shown in Supplemental Fig. S1. We probed blots with EBV-positive reference human serum and detected an 82-kDa band, indicative of wtEBNA1 (Akata strain [37]), only in cells inoculated with Adv5-CV-AKE1, which served as the positive control. On the same blots, we detected a signal band at around 21 kDa, the expected molecular size of mtEBNA1, in cells inoculated with Adv5-CV-DNE1 but not with Adv5-CV-LacZ (Supplemental Fig. S1). The 21-kDa band was also produced by clones of Adv5-SV-DNE1, Adv5/35f-CV-DNE1, and Adv5/35f-SV-DNE1 (data not shown). Neither the 21-kDa nor the 82-kDa protein was detectable when probed with EBV-negative human serum (data not shown).

Reduction of Episome-Derived wtEBNA1 Expression and EBV Genomic Loads by mtEBNA1 Transduction

We analyzed the effects of mtEBNA1 using EBV-converted or -reinfected cell lines (Table 1), which had been established *in vitro* by infecting virus-negative cells with recombinant EBV (rEBV; Akata strain) that carries the neomycin-resistance gene (*neo*^{r}) as a selective marker [38]. For example, we cultured the rEBV-converted epithelial cell line NU-GC-3/rEBV [39] in the absence of G418 for 7 days and inoculated it with Adv5-CV-DNE1 and monitored the expression of both rEBV episome-derived wtEBNA1 and transduced mtEBNA1 proteins by immunoblotting. The 21-kDa mtEBNA1 protein was detectable at least for 9 days after Adv inoculation (Fig. 2A). Concomitantly, expression of wtEBNA1 prominently declined with time

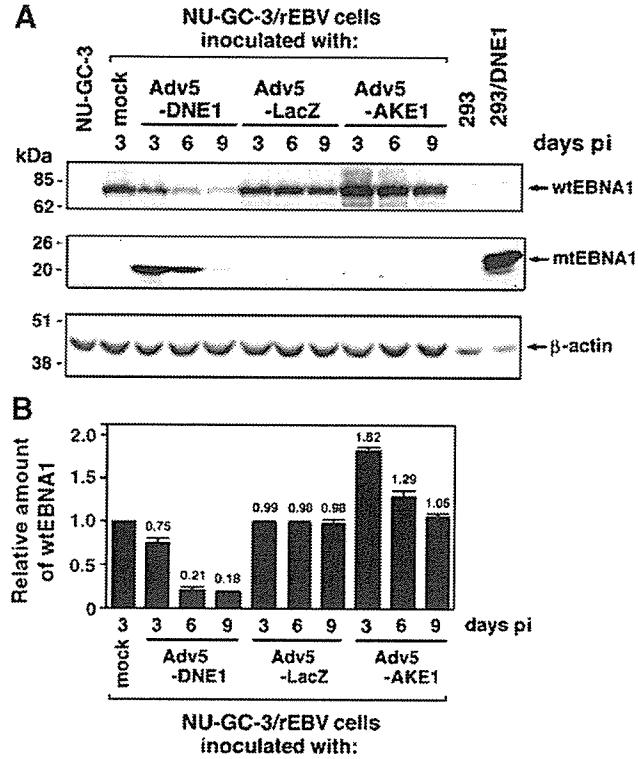

FIG. 2. Sequential decrease in rEBV episome-derived wtEBNA1 expression by mtEBNA1 transduction. (A) Immunoblot. Representative data from one of three experiments using the epithelial converted cell line NU-GC-3/rEBV are shown. Cells were inoculated with CsCl-purified Adv5-CV-DNE1 or -LacZ or -AKE1 (m.o.i. of 20) and cultured without G418. Expression of wtEBNA1 (top row), mtEBNA1 (second row), and β-actin (third row) was assayed at the days indicated postinoculation (pi). The cell lines 293 and 293/DNE1 served as mtEBNA1-negative and -positive cell controls, respectively (see Materials and Methods). Molecular size standards are indicated at the left. (B) Quantification of wtEBNA1 expression levels. Bands specific for wtEBNA1 were analyzed quantitatively in comparison with β-actin signals. Expression levels of wtEBNA1 protein in the Adv5-CV-DNE1- or Adv5-CV-LacZ-inoculated NU-GC-3/rEBV cells were expressed as relative values against a mock-infected control. Black columns with bars represent means ± SD of results from three repeated experiments.

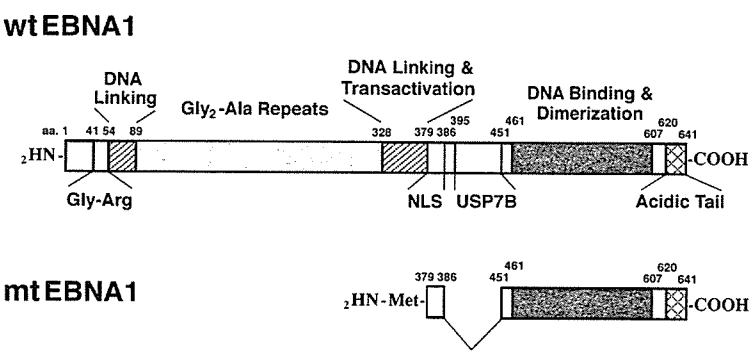

FIG. 1. Structure of mtEBNA1 used in this study. Functional domains of the mtEBNA1 are schematically diagramed in comparison with wtEBNA1. Amino acid coordinates are indicated above the limits (vertical bars) of each domain according to the published data [22,30,34]. The coding constructs of mtEBNA1 and wtEBNA1 (LacZ and EGFP, too), which are transcribed by SVp or CMVp, were incorporated into Adv5 or Adv5/35f. NLS and USP7B indicate nuclear localization signal [22] and putative ubiquitin-specific protease 7 binding domain [30], respectively.

(Fig. 2A). A quantitative analysis, normalized to β-actin levels, demonstrated that wtEBNA1 expression from Adv5-CV-DNE1 inoculation, but not in Adv5-CV-LacZ inoculation, decreased to 75 and 18% of the mock-inoculated control 3 and 9 days after inoculation, respectively ($P < 0.01$, analyzed by ANOVA, followed by the post hoc Tukey test) (Fig. 2B). We also observed a similar reduction in wtEBNA1 in other rEBV-reinfected and -converted lym-

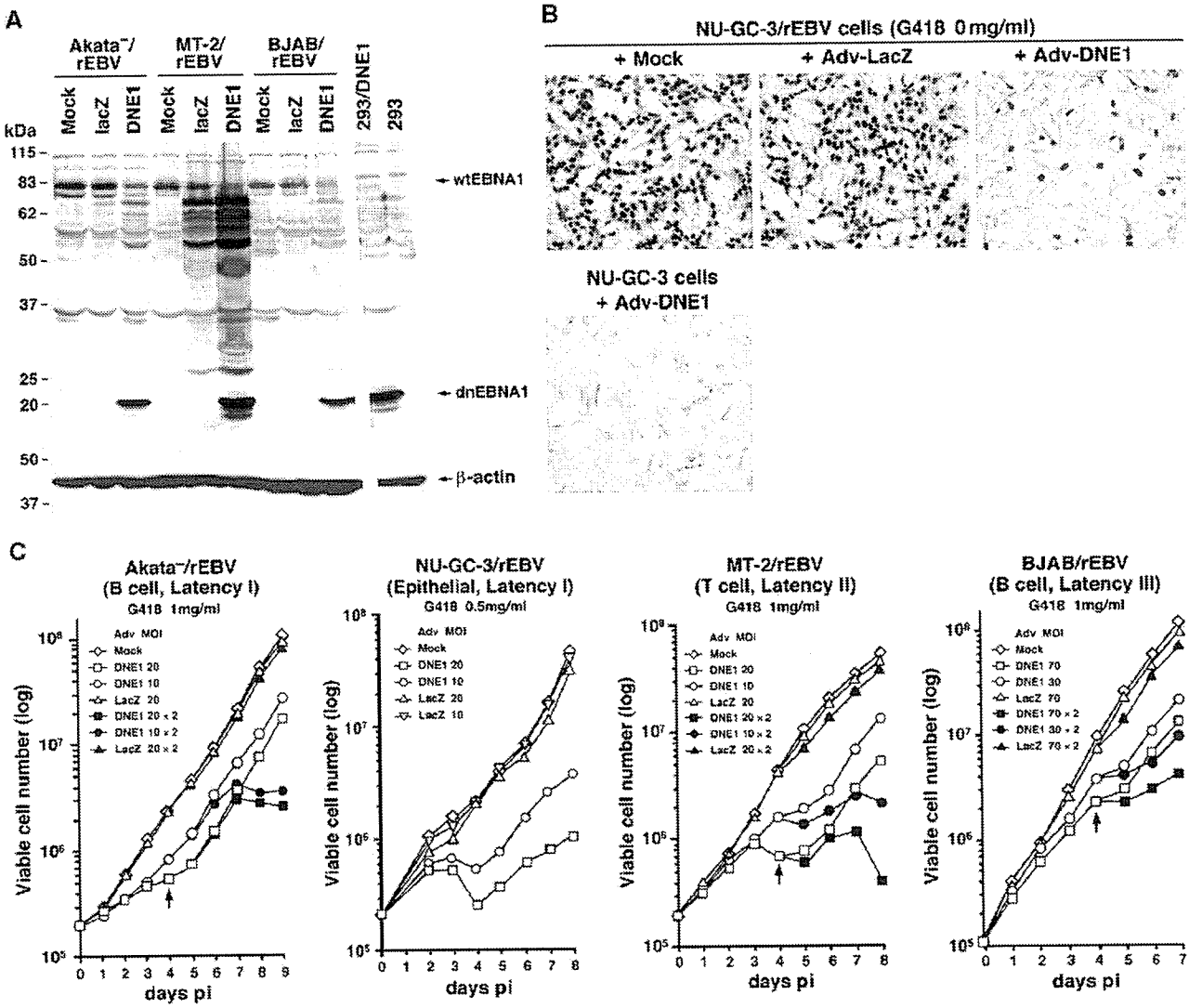

FIG. 3. Complete eradication of EBV episomes by dnEBNA1 at the single-cell level regardless of latency type and cell type. (A) Expression of dnEBNA1 in other rEBV-converted cell lines. Substantial expression of dnEBNA1 (hereafter, our mtEBNA1 is referred to as "dnEBNA1," see text) in rEBV convertants of different EBV latency types and cell lineages (Table 1). Results from Akata⁻/rEBV, MT-2/rEBV, and BJAB/rEBV are shown. The convertants were inoculated with Adv5-SV-DNE1 at an m.o.i. of 20 for Akata⁻/rEBV and MT-2/rEBV and 70 for BJAB/rEBV and cultured without G418. Immunoblot analysis was carried out 3 days postinoculation. Obvious 21-kDa bands, indicative of dnEBNA1, and a decrease in 82-kDa bands representing wtEBNA1 were unequivocally seen only in Adv5-SV-DNE1-inoculated cells. Several accentuated extra bands, particularly visible in MT-2/rEBV cells exposed to Adv, could represent adenovirus-related proteins that reacted with human serum used as the probe. Detection of β-actin levels served as the internal control. The negative and positive controls, 293 and 293/DNE1, respectively, are the same as explained in the Fig. 2A legend. Molecular size standards are indicated on the left. (B) EBER1-ISH. Representative data from a series of NU-GC-3/rEBV cells are shown. The cells were inoculated with Adv's at an m.o.i. of 20 and cultured in the absence of G418. The incidence of rEBV loss was assessed by EBER1-ISH 9 days after inoculation. Cells with strong nuclear signals are EBER1-positive. NU-GC-3 + Adv5-DNE1 served as a rEBV-negative control. Fine granular precipitates visible in the background of Mock and Adv5-LacZ samples of NU-GC-3/rEBV are nonspecific products that occasionally appear during the final chromogenic reaction step. Original magnification: ×100. (C) Growth kinetics of dnEBNA1-transduced rEBV convertants in the presence of G418. Adv5-CV-DNE1 or -LacZ was used for NU-GC-3/rEBV and Adv5-SV-DNE1 or -LacZ was used for the other convertants. The Adv's and applied m.o.i. are indicated by abbreviations and Arabic numerals, respectively, and are attached to the symbols. In Akata⁻/rEBV cells, for example, DNE1 20 represents a single Adv5-SV-DNE1 inoculation at an m.o.i. of 20, and DNE1 20 × 2 represents repeated Adv5-SV-DNE1 inoculations at an m.o.i. of 20. The second Adv inoculation is indicated by an arrow. Viable cells were consecutively counted by trypan blue dye exclusion. Data from one of two independent experiments are provided here.